# Geospatial Assessment of United States Tropical Cyclone Disaster Risk

**Stephen M Strader**

stephen.strader@villanova.edu

Villanova University https://orcid.org/0000-0002-6472-3182

**Sydney J Walsh**

Villanova University

**Thomas M Linehan**

Villanova University

**Caroline M Carlson**

Villanova University

**Research Article**

**Keywords:** Tropical Cyclone, Hazard, Disaster, Vulnerability, Exposure, Resilience

**Posted Date:** October 27th, 2025

**DOI:** https://doi.org/10.21203/rs.3.rs-7594168/v1

**Geospatial Assessment of United States Tropical Cyclone Disaster Risk**

Stephen M. Strader[1*], Sydney J. Walsh[1], Thomas M. Linehan[1], and Caroline M. Carlson[1]
[1]Department of Geography and the Environment, Villanova University

*Corresponding author address: Stephen M. Strader, Dept. of Geography and the Environment, Villanova University, Villanova, PA 19085
E-mail: stephen.strader@villanova.edu
ORCiD: 0000-0002-6472-3182

**Abstract**

This study provides an overview of tropical cyclone (TC) hazard risk, population exposure, societal vulnerability, and community resilience for conterminous United States (CONUS) counties. TC hazard and disaster indices developed in this work combine measures of hazard risk ($TC_{HR}$), exposure ($TC_{EXP}$), vulnerability ($TC_{VUL}$), resilience ($TC_{RES}$), and disaster risk (TCDR) to determine the counties that are most likely to experience TC hazard impacts and suffer from a disaster. Results from this research indicate that counties in Florida, Louisiana, North Carolina, and southeastern Texas are most prone to TC disasters. Harris and Cameron, TX Counties rank highest of all counties in terms of TC disaster risk. Whereas TC disaster potential is largely greater for Atlantic and Gulf Coast counties because of a combination of high TC hazard incidence and population exposure, many inland or non-coastal counties across the southeastern and northeastern CONUS are also highly disaster prone due to frequent inland flash flooding from landfalling TCs being juxtaposed vulnerable communities. Geospatial patterns in TC hazards and fatalities in relation to the underlying population exposure, vulnerability, and resilience are critical for understanding how the next TC disaster may unfold. In all, outcomes from this research are aimed at improving local, state, and federal stakeholder (e.g., emergency managers, policymakers, land use planners) knowledge about the various threats their communities face from TCs. Our findings may assist officials with developing TC hazard-specific mitigation and resilience-building strategies with the ultimate goal of reducing casualties and losses from future TCs.

**Keywords**: Tropical Cyclone, Hazard, Disaster, Vulnerability, Exposure, Resilience

## 1 Introduction

Over the last decade, conterminous United States (CONUS) tropical cyclones (TCs; tropical storms and hurricanes) have caused over $820 billion dollars (USD) in losses (NOAA 2025). In 2017 alone, TCs were responsible for nearly $340 billion dollars in losses and 3,167 direct fatalities, making it the most costly and deadly CONUS TC season in the last four decades (NOAA 2025). While TC impacts and fatalities are most commonly linked to the larger parent storm, the hazards TCs produce are the root causes of deaths and damage. TC hazards include inland precipitation that can lead to freshwater and/or flash flooding, coastal storm surge, damaging winds, rip currents, dangerous offshore marine conditions, and tropical cyclone tornadoes (TCT). In this study, we examine the intersection and relationships between these six deadly TC hazards and society. A county-level assessment of TC disaster risk is generated through geospatial analyses and the creation of disaster indices incorporate measures of TC hazard incidence, population exposure, societal vulnerability, and community resilience. This research is aimed at providing a baseline assessment of where TC disasters are most likely to occur. Our primary goal is to help stakeholders better understand the TC hazards that are most likely to impact exposed and vulnerable communities, creating disasters. Findings from this work will help emergency managers, land use planners, and policymakers develop, improve, and institute fatality- and impact-reducing strategies before, during, and after TCs make landfall. In addition, this findings from this study will assist future work aimed at developing mitigation, adaptation, response, and recovery strategies for the most TC disaster-prone counties.

## 2 Background

Several prior studies have examined the relationships between TC hazard incidence, atmospheric conditions, and societal impacts (Rappaport 2000; Muller and Stone 2001; Senkbeil

et al. 2011; Rappaport 2014; Fussell et al. 2017; Xi and Lin 2022; Lamers et al. 2023). These studies have mostly concentrated on spatial and temporal patterns in TC hazard incidence and severity, finding that many communities and populations in coastal and southeastern CONUS regions are threatened by multiple TC hazards each year (Peduzzi et al. 2012; Moore et al. 2017; Tennille and Ellis 2017; Sajjad et al. 2020; Summers et al. 2022). Others have focused on TC hazards as they relate to mortality, indicating that water hazards such as inland flooding and storm surge are the direct cause of most TC fatalities in the CONUS (Rappaport 2000; Rappaport 2014; Rappaport and Blanchard 2016; Parks et al. 2022; Young and Hsiang 2024). Research has illustrated that inland flooding and storm surge are of greatest concern since they have been responsible for more than 75% of historical CONUS TC deaths (Rappaport 2014). Nearly one quarter of all landfalling TCs cause a fatality, with approximately 50 people being killed each year on average by TC hazards (Rappaport 2014). Past research examining the relationships between TC hazards and disasters has shown that societal factors related to exposure, vulnerability, and resilience are also critical when assessing TC hazard impacts and disasters (Schmidt et al. 2010; Morrow and Lazo 2015; Pilkington and Mahmoud 2017; Krichene et al. 2023; Gori et al. 2025). Thus, a large portion of research on TC disasters has been dedicated to creating and improving community resilience-building strategies aimed at reducing TC losses (Lumbroso et al. 2017; Pilkington and Mahoud 2017; Mendelsohn and Zheng 2020).

Most TC hazard studies concentrate their efforts on individual TC hazards. Many past studies have focused on inland precipitation because the impacts from flooding tend to be widespread and costly (Atallah et al. 2007; Knight and Davis 2009; Kunkel et al. 2010; Villarini et al. 2014; Zick and Matyas 2016; Touma et al. 2019; Maxwell et al. 2021). Additional work on storm surge (Needham and Keim 2012; Needham and Keim 2014; Needham et al. 2015; Resio

and Irish 2015; Zachry et al. 2015; Rahmstorf 2017; Booth et al. 2021; Towey and Booth 2022), wind (Cui and Caracoglia 2016; Mudd et al. 2017; Tan and Fang 2018; Henry et al. 2020; Song and Chung 2024), rip currents and dangerous off shore marine conditions (Gensini and Ashley 2010; Paxton and Collins 2014; Rappaport 2000), and TCTs (Gentry 1983; Schultz and Cecil 2009; Edwards 2012; Moore and Dixon 2012; Paredes et al. 2021) has also been conducted, revealing differences in TC hazard incidence location and severity relative to TC characteristics and the underlying society. Compounding effects of TC hazards have also been assessed in past research (Pilkington and Mahmoud 2017; Trepanier et al. 2017; Sheng and Hong 2020; Gori et al. 2022; Tonn and Czajkowski 2022). These investigations found that TC hazards tend to occur simultaneously with other hazards (e.g., inland flooding and TCTs, storm surge, and wind), creating issues regarding protective action decisions and evacuation (Nielsen et al. 2015).

TC hazard research has taken several methodological approaches at varying spatial and temporal scales. Some studies have assessed patterns in TC precipitation and inland flooding as they relate to storm intensity, storm evolution, and the underlying landscape characteristics (e.g., land use, land cover, soil moisture conditions, river and stream levels; Senkbeil et al. 2011; Villarini et al. 2014). Others have concentrated on spatial patterns in TC hazard impacts as they relate to society. These works have illustrated that while storm surge, rip currents, and dangerous offshore marine conditions are inherently linked to coastal regions of the CONUS, TC hazards such as extreme rainfall, damaging wind, and TCTs often affect communities far removed from coastal regions (Rezapour and Baldock 2014; Liu and Smith 2016; Van Oldenborgh and Van Der Wiel 2017; Varlas et al. 2019).

Some researchers have examined societal exposure, vulnerability, and resilience relative to TCs to better understand potential impacts, disasters, and mortality for many eastern CONUS

93 regions, including the Atlantic and Gulf Coasts (e.g., Freeman and Ashley 2017; Pilkington and
94 Mahmoud 2017; Anderson et al. 2020; Mendelsohn and Zheng 2020; Parks et al. 2022; Swain
95 and Bellino 2022; Wilson et al. 2022; Jing et al. 2024). Societal exposure is defined as persons,
96 property, and/or the things society values that are subject to hazard impacts and losses (UNDRR
97 2017a). Vulnerability has many definitions, but it is most often described as the susceptibility of
98 people or a system to damage or harm, encompassing elements of exposure (i.e., people, assets,
99 or characteristics of the natural and/or built environment that position a system to be affected by
100 a hazard), sensitivity (i.e., degree to which a community or system is affected by hazard
101 conditions), and adaptive capacity (i.e., ability for a community or system to cope or adapt to
102 hazard conditions; UNDRR 2017b). Resilience is related to the ability of a person, community,
103 or system to resist, absorb, adapt to, transform, and recover from the effects of a hazard in a
104 timely and efficient manner (UNDRR 2017c). Each of these variables can be combined to
105 generate a measure of disaster risk (Thywissen 2006; UNDRR 2017d). Disaster risk is defined as
106 the potential for loss of life, injury, and/or severe damage from a hazard that causes substantial
107 disruption to the essential functions of a society, community, or system and threatens its ability
108 to cope without external assistance (UNDRR 2017d). Although various definitions exist across
109 the hazards and disaster sciences, disaster risk is largely a function of hazard incidence,
110 exposure, vulnerability, and resilience (Thywissen 2006).
111 The disaster risk of a community or region is often assessed through the creation and
112 implementation of an index or indices (e.g., Kaly et al. 1999; Peduzzi 2006; Peduzzi et al. 2009;
113 Cutter et al. 2010; Flanagan et al. 2011; Cutter et al. 2014; Strader and Ashley 2018; Cutter
114 2024; Painter et al. 2024). An index within the hazards and disasters research field is a composite
115 statistic that combines multiple indicators, whether they be related to the hazard or society, to

generate a composite score that pertains to the specific index topic such as disaster risk. Hazard and disaster indices combine physical (e.g., hazard frequency, magnitude, location) and/or social (e.g., population density, poverty, age, housing type) measures within a mathematical framework to calculate a representative value that directly relates to the disaster frequency and severity within a specific geography (e.g., country, state, county). Studies have applied index methods to evaluate TC risk for coastal communities in the CONUS and around the world (e.g., Davidson and Lambert 2001; Bjarnadottir et al. 2011; Xiao et al. 2011; Bobby 2012; Hernandez et al. 2018; Helderop and Grubesic 2022; Do and Kuleshov 2023; Song and Chung 2024). The application of indices to assess TC risk and associated hazards is diverse, ranging from the national to local scale and incorporating a variety of social and physical factors that control TC disaster risk.

## 3 Data and Methods

TC hazard data were gathered from a variety of public sources such as National Oceanic and Atmospheric Administration (NOAA), National Hurricane Center (NHC), and Federal Emergency Management Agency (FEMA). We analyze spatial patterns in TC hazard incidence for each of the six most common TC fatality causes (i.e., inland flash flooding, coastal storm surge, damaging winds, rip currents, dangerous offshore marine conditions, and TCTs), resulting in county-level enumerations of where TC hazards are most frequent. These measures are then combined with metrics related to societal exposure, vulnerability, and resilience to determine the counties that are at greatest risk to TC disasters.

### 3.1 Direct Tropical Cyclone Fatalities

We first assess direct fatality causes by TC hazard type from 2005 to 2024 to determine the TC hazards that are most likely to result in deaths (NHC 2025). This time period was selected

because it aligns with available TC hazard data availability (i.e., precipitation data). These data were gathered from NHC's tropical cyclone reports that provide comprehensive overviews of TC events, including information on casualties. By going storm-by-storm within, we were able to determine the number, cause, and location of TC deaths over the 20-year study period. Fatalities were stratified by each hazard type with the proportion of total TC fatalities from 2005 to 2024 by TC hazard type being used in a TC disaster risk index calculation that is discussed in the last section of our methods.

### 3.2 Inland Flash Flooding

To examine TC inland flash flooding, we developed a methodology for determining the amount and location of heavy rainfall from past TCs as they approached and traversed the CONUS. We first downloaded TC track data from the NCEI's International Best Track Archive for Climate Stewardship (IBTrACS version 4). This dataset contains the best TC track position of past events at 3-hour intervals and storm information such as seasonal timing, location, ocean basin, track status (e.g., tropical depression, tropical storm, hurricane), maximum sustained wind speed, wind radii, central pressure, and distance to land (Knapp et al. 2010). For a TC track to be included in the inland precipitation and flooding analysis, it had to meet three criteria: 1) achieve tropical storm status within 600 km of the CONUS, 2) occur within the North Atlantic Ocean Basin, and 3) take place from 2005 to 2024. Tracks not within 600 km of the CONUS were excluded from analyses given prior research has illustrated that it is relatively uncommon for precipitation to be associated with a TC beyond 600 km of the storm center (Kirkland and Zick 2019).

Once TC tracks within 600 km of the CONUS were compiled, we then turned to NOAA Quantitative Precipitation Estimate (QPE) data from the Advanced Hydrologic Prediction

Service (AHPS) to gather precipitation estimates associated with each TC track included in our study. QPE data are derived from a combination of satellite, radar, and rain gauge measurements of precipitation and was developed through a partnership between the NWS River Forecast Centers (RFCs) and the National Centers for Environmental Prediction (NCEP; NWPS 2025). AHPS combines these precipitation measures to generate daily (24-hr) raster estimates of total precipitation across the CONUS at 4-km gridded spatial resolution. Stage IV QPE data were employed for the 2016 through 2024 time period, while Stage III QPE data covered the 2005 through 2015 analysis period. For precise details on APHS QPE data creation see NWPS (2025).

We matched the date from when the TC first comes within 600 km of the CONUS to the underlying 24-hr QPE data for the same date to determine the precipitation location and magnitude associated with each TC track. We then downloaded the 24-hr QPE data for each subsequent day as long as the TC was within 600-km of the CONUS. This daily QPE data gathering process continued until the TC either dissipated or moved outside of the 600-km CONUS buffer zone. TC QPE days ranged from a single day to over a week for some storms (e.g., Hurricane Harvey).

Because not all precipitation from TCs leads to flash flooding, we also applied a 24-hr total precipitation threshold for each daily QPE raster. Prior research has indicated that flash flooding is most often associated with precipitation totals of 50.8 mm (2 inches) or greater within a 24-hour period (Huang et al. 2022). While we recognize that flash flooding is also dependent on several other factors such as precipitation duration, precipitation intensity, land use, land cover, etc. (Marchi et al. 2010; Sohn et al. 2020), the 50.8-mm threshold was the best compromise for the analyses in this study given the spatial and temporal scale limitations of the QPE dataset versus lengthy historical period of TC events we examined. In all, the 50.8 mm and

greater 24-hour precipitation threshold provides a conservative measure of inland flooding potential or specifically, TC flash flooding (TCFF) precipitation within each 4-km QPE grid cell.

Lastly, because not all precipitation during the timeframe when the TC is traversing the CONUS is associated with the TC, we removed any TCFF precipitation grid cells that were not within 600 km of the TC centerline or track. All TCFF precipitation grid cells were then intersected with the underlying county and aggregated to provide a county-level measure of TCFF potential (i.e., mean total precipitation from ≥50.8 mm TCFF grid cells). County-level estimates were then ranked to yield a relative measure of TCFF potential compared to all other CONUS counties. In all, this methodology resulted in 122 TC events (61 tropical storms and 61 hurricanes) from 2005 to 2024 that produced TCFF precipitation within the CONUS.

### 3.3 Coastal Storm Surge

Coastal storm surge was examined through NOAA's Sea Lake and Overland Surges from Hurricanes (SLOSH) model (Jelesnianski et al. 1992). SLOSH is a numerical model that estimates maximum storm surge inundation from hurricanes that make landfall along the CONUS Gulf and East Coasts. SLOSH was developed in collaboration with FEMA, NWS, and the U.S. Army Corps of Engineers (USACE) by using historical hurricane events and associated storm surge observations. The SLOSH model considers hurricane central pressure, size, forward (translational) speed, track, sustained wind speeds, wind radii, and the coastal topography to estimate potential maximum storm surge by landfalling location and hurricane intensity (i.e., Category 1 through 5; Zachry et al. 2015). The NHC currently employs the SLOSH model using over a dozen basins along the Atlantic and Gulf Coasts in conjunction with a sample of hypothetical hurricanes to estimate a near worst-case scenario of storm surge flooding by hurricane intensity (Zachry et al. 2015). These data are referred to as the National Storm Surge

Risk Maps Version 3. For specific details on the history and development of SLOSH see Glahn et al. (2008).

Storm surge risk data was downloaded from the NHC in raster (GeoTIFF) format for all coastal locations stretching from Texas to Maine and for hurricane categories 1 through 5. This process resulted in five rasters that represent potential maximum storm surge by hurricane intensity. The storm surge grid cells were then aggregated to the associated or intersecting coastal county to provide a county-level measure of maximum potential storm surge by hurricane intensity. This method is similar to the TCFF precipitation grid cell-county aggregation methodology discussed in the prior. Lastly, the county-level storm surge estimates were then averaged across all hurricane intensities to represent a measure of mean maximum storm surge inundation for all hurricanes and intensities.

### 3.4 Severe Wind, Rip Currents, and Dangerous Offshore Marine Conditions

We use FEMA's National Risk Index (NRI) data as a means of TC hazard incidence information related to TC winds, rip currents, and dangerous offshore marine conditions. FEMA developed the NRI to highlight communities that are at risk from a set of 18 natural hazards (FEMA 2025). NRI TC data provided us with a measure of historical TC event frequency for all CONUS counties. The process for determining county-level TC frequency involved employing the NOAA NCEI HURDAT2 Best Track Data Archive that contains historical TC observations from 1851 to 2020. These data are equivalent to the IBTrACS data discussed in the above inland flooding methods section. The NRI working group applied a geospatial buffering method on HURDAT2 data to approximate TC size, intensity, and location as the storm evolved over time. Specifically, HURDAT2 TC line segments that make up the TC track were buffered by the TC wind radii at regular time intervals to estimate areal TC coverage as the storm traversed open

231 water and after making landfall (c.f. Figures 71and 72 in FEMA 2025). Each buffered TC track
232 was then intersected with CONUS counties to yield a county-level measure of TC incidence. The
233 TC wind incidence estimates are solely the product of the number of times TC winds traversed a
234 county from 1851 to 2020.

235 Because rip currents and dangerous offshore marine conditions are often directly related
236 to TCs as they are near and/or make landfall along the Gulf and East Coasts, we also use the NRI
237 TC incidence data to represent rip current and offshore marine hazards during TC events. The
238 difference between county-level TC wind and rip current and offshore marine incidence data
239 utilized in our study is that TC winds can traverse well inland, intersecting non-coastal counties,
240 while rip current and offshore marine threats are isolated to those coastal counties that have
241 access to open ocean water. Therefore, we only consider counties that have access to the open
242 ocean (Gulf of Mexico and Atlantic Ocean) to be at risk for rip currents and dangerous offshore
243 marine conditions.

244 **3.5 Tropical Cyclone Tornadoes**

245 Tornadoes associated with TCs have been archived by the NOAA Storm Prediction
246 Center (SPC) from 1995 to 2024 (SPC 2024). SPC's TCT database contains information on all
247 tornadoes associated with TCs including TCT location (latitude, longitude), damage magnitude
248 or intensity (Enhanced Fujita Scale 0-5; McDonald et al. 2009), casualties, distance from the TC
249 center, time and date, and location and bearing information relative to the TC center. For our
250 study, we plot the tornado damage path (polyline) using the starting and ending location of each
251 TCT and aggregate them to the underlying county or counties that the tornado traversed. The
252 resulting county-level tornado count from 1995 to 2024 is then used to estimate TCT incidence
253 across the CONUS.

### 3.6 Exposure, Vulnerability, and Resilience

American Community Survey (ACS) 5-year total population estimates were used as a measure of societal exposure to TC hazards. County-level ACS 5-year total population estimates covering the period of 2018 to 2023 were downloaded from the National Historical Geographic Information System (NHGIS; Manson et al. 2024). These data contain total population estimates as well as margin of error for county enumerations. We use the total population value to represent the number of people within a county that could potentially be exposed to a TC hazard.

The CDC's Social Vulnerability Index (SVI) for the year 2022 (most recent year available) was used to estimate county-level vulnerability across the CONUS (Flanagan et al. 2011). This dataset considers 16 societal metrics that have been shown to indicate how vulnerable a person or community is to natural hazard impacts and disasters. Each of the SVI vulnerability metrics are grouped into four categories: socioeconomic status, household characteristics, racial and ethnic minority status, and housing type and transportation (Flanagan et al. 2011). For the socioeconomic status category, factors such as poverty, employment status, housing cost, education, and healthcare are considered. Household characteristic vulnerability metrics are associated with population age, disability, marital status, and language proficiency. The racial and ethnic minority status category directly relates to minority populations, and the housing type and transportation grouping is comprised of metrics related to multi-unit housing structures, manufactured homes, crowding, no vehicle access, and group quarters. In all, these 16 variables are used to create four categorical estimates of vulnerability and an overall vulnerability score for all CONUS counties. For more information on the development of the SVI see Flanagan et al. (2011).

County-level resilience data was downloaded from the FEMA NRI (FEMA 2025). FEMA NRI derived the resilience data from the Hazards and Vulnerability Research Institute (HVRI) Baseline Resilience Indicators for Communities (HVRI BRIC) index. The HVRI BRIC dataset uses a set of 49 indicators that help determine how resilient a county is to natural hazards. Each of the 49 indicators is grouped into one of six categories of resilience: social, economic, community capital, institutional capacity, housing and infrastructure, and environmental. These six categories help determine how well a community (county) is able to prepare for, withstand, and recover from natural hazards. County population, vulnerability, and resilience scores are percentile ranked to determine those that are above or below the CONUS average (median; 50$^{th}$ percentile) score.

### 3.7 Tropical Cyclone Disaster Indices

Using the aforementioned county-level TC hazard incidence, population exposure, societal vulnerability, community resilience, and TC fatality statistics, we created several indices to determine the CONUS counties that are most likely to experience and suffer from TC hazards and associated impacts. We first created a fatality-weighted TC hazard risk index ($TC_{HR}$; **Eq. 1**) that uses the proportion of all TC fatalities from 2005 to 2024 by TC hazard type to weight the county-level percentile ranking value for each TC hazard category. The $TC_{HR}$ index does not assume that all TC hazards are of equal importance; rather, those TC hazards that have historically killed greater numbers of people are emphasized in the TC hazard risk index. The values for $TC_{HR}$ index calculations are then ranked for each CONUS county, providing a relative measure of county-level TC hazard occurrence or risk.

$$TC_{HR} = (fatality\ \%)(Inland\ Flooding\ Pct\ Rank) + (fatality\ \%)(Storm\ Surge\ Pct\ Rank) + (fatality\ \%)(Wind\ Pct\ Rank) + (fatality\ \%)(Rip\ Current\ and\ Offshore\ Marine\ Pct\ Rank) + (fatality\ \%)(TCT\ Pct\ Rank)$$

***Eq. 1***

Our TC hazard exposure index combines county-level TC hazard incidence with total county population estimates to determine population exposure to potential TC hazards ($TC_{EXP}$; **Eq. 2**). $TC_{EXP}$ index scores are generated by multiplying county $TC_{HR}$ percentile rankings by county percentile rankings for total population as derived from 5-year (2018-2023) ACS county-level population enumerations. Each county-level $TC_{EXP}$ score is then percentile ranked, providing a relative estimate of societal exposure to TC hazards across the CONUS.

$$TC_{EXP} = (TC_{HR})(Total\ Population) \qquad \textbf{\textit{Eq. 2}}$$

Because vulnerability is a function of the underlying societal exposure, hazard incidence, and other societal factors such as income, age, education, etc., we combine $TC_{EXP}$ measures with county-level CDC SVI scores to create a TC vulnerability index ($TC_{VUL}$; **Eq. 3**). $TC_{VUL}$ values are calculated by multiplying the county-level $TC_{EXP}$ index percentile rankings with the CDC SVI county-level vulnerability percentile rankings. The resulting $TC_{VUL}$ index values are then ranked to provide a relative county-level measure of TC hazard vulnerability across the CONUS.

$$TC_{VUL} = (TC_{EXP})(Vulnerability) \qquad \textbf{\textit{Eq. 3}}$$

Community or county TC disaster resilience is calculated through an index that combines county-level percentile rankings for $TC_{EXP}$ and county-level rankings for community resilience derived from the HVRI BRIC ($TC_{RES}$; **Eq. 4**). As mentioned prior, because county-level resilience percentile rankings from the HVRI BRIC are ranked from most resilient ($100^{th}$ percentile) to least resilient ($1^{st}$ percentile), we multiply county $TC_{EXP}$ by one minus the county-level HVRI BRIC resilience percentile ranking value. The $TC_{RES}$ scores are again ranked to provide a comparative representation of TC hazard resilience at the county scale. This index signifies those heavily populated counties where community resilience is low and TC hazard incidence is high.

$$TC_{RES} = (TC_{EXP})(1 - Resilience) \quad \textbf{\textit{Eq. 4}}$$

Lastly, we developed a TC disaster risk index (TCDR) that considers TC hazard incidence, population exposure, social vulnerability, and community resilience (**Eq. 5**). This index multiplies TC hazard incidence ($TC_{HR}$), ACS total county population enumerations, CDC SVI vulnerability, and HVRI BRIC community resilience scores to generate a county-level score that relates to potential TC disaster risk. As with $TC_{HR}$, $TC_{EXP}$, $TC_{VUL}$, and $TC_{RES}$ index scores, the TCDR county scores are percentile ranked and mapped to illustrate potential TC disaster risk across the CONUS. Higher percentile rankings for TCDR indicate a more disaster-prone county.

$$TCDR = (TC_{HR})(Total\ Population)(Vulnerability)(1 - Resilience) \quad \textbf{\textit{Eq. 5}}$$

## 4 Results

### 4.1 Tropical Cyclone Fatalities

Our TC fatality dataset contains 61 tropical storms and 61 hurricanes that produced hazards across the CONUS from 2005 to 2024 (**Figure 1a**). These 122 TC events were the direct cause of 1,306 deaths over the last two decades (**Figure 1b**). Louisiana has experienced the greatest number of direct TC hazard deaths with 368 over the 20-year study period, followed by Florida (179), North Carolina (159), Mississippi (179), and Texas (121; **Figure 1c**). Only 43 TC hazard deaths occurred in non-costal states, with Tennessee containing the greatest number of fatalities from 2005 to 2024 at 15 deaths. Only one coastal state (Massachusetts) did not experience a direct TC fatality over the 20-year period.

Storm surge has killed the most people (640) since 2005, followed by inland flooding (375) and severe winds (187). Hurricane Katrina in 2005 was responsible for 80% (513 of 640) of all storm surge fatalities in our 20-year analysis, while Hurricane Helene in 2024 was responsible for 25% (95 of 375) of direct inland flood fatalities (**Figure 1c**). The highest

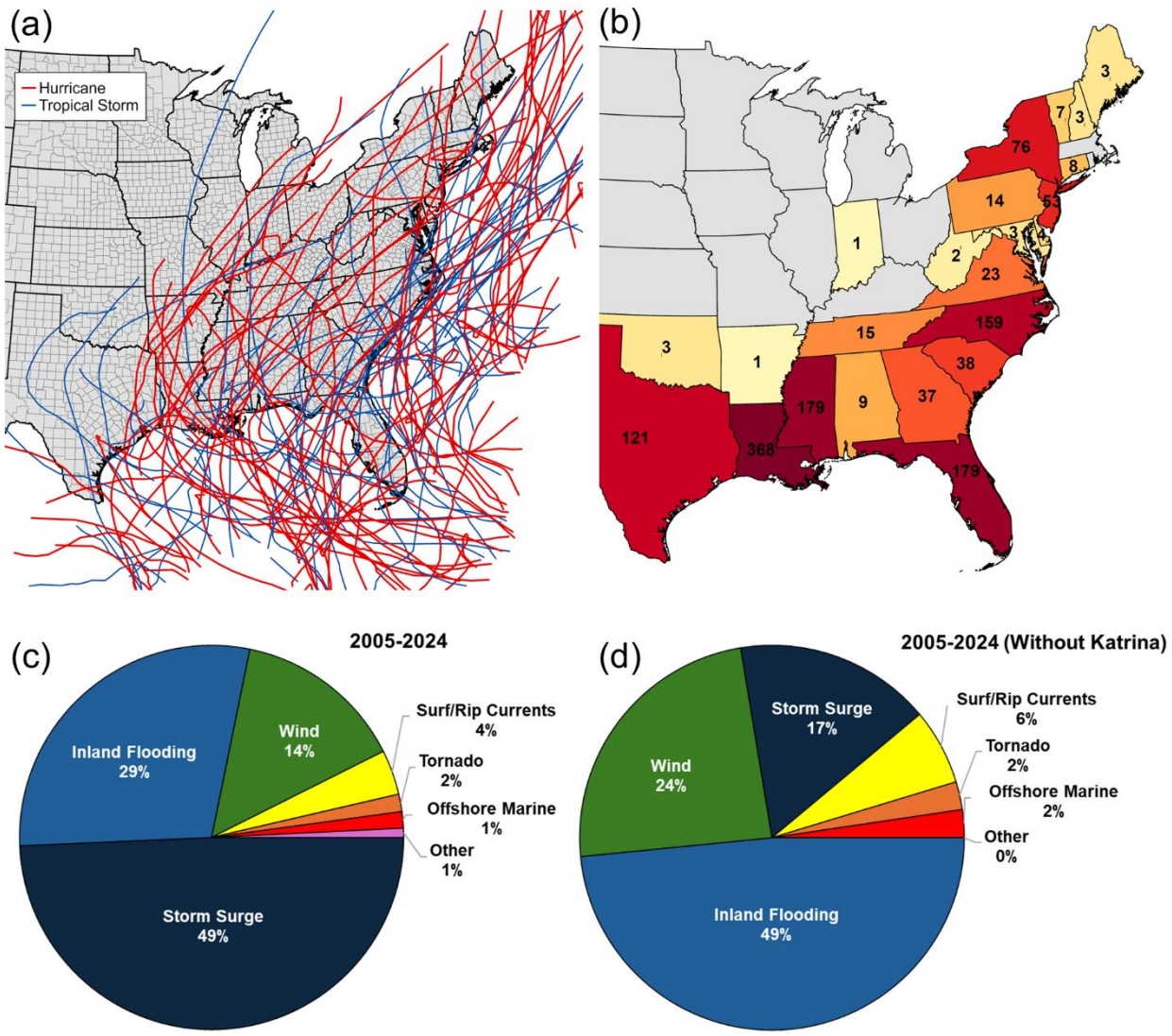


**Fig. 1** Panel (a) indicates the TCs that tracked within 600 km of the CONUS coast from 2005 to 2024. Panel (b) represents the total number direct TC deaths by state from 2005 to 2024. Pie charts denote the proportion direct fatalities by TC hazard type from 2005 to 2024 (c) with and (d) without considering Hurricane Katrina's direct fatalities.

proportion of wind fatalities (65 of 187) over the 20-year study period was also associated with Hurricane Helene. Other TC hazards such as rip currents, offshore marine, and TCTs have killed a collective 86 people since 2005, with most (49) of the deaths being attributed to rip currents. There were also 10 direct TC fatalities where the deaths could not be attributed to a specific TC

hazard. Taking all TC hazard fatality causes into account, storm surge, inland flooding, and wind were collectively the direct cause of 92% of all TC fatalities since 2005.

Past research has illustrated that Hurricane Katrina's impacts on New Orleans, LA were a function of physical, infrastructural, and societal factors (e.g., Cutter and Gall 2006; Jonkman et al. 2009; Shaffer et al. 2009; Boyd 2010). From a physical standpoint, Katrina was an intense Category 3 hurricane as it made landfall. Its forward speed, strong winds, bearing, and landfalling location allowed it to generate storm surge up to 8.5 meters (28 feet). Many failed levees such as those surrounding The Mississippi River Gulf Outlet (MRGO) also played a critical role in creating the disaster by exacerbating the storm surge from the Gulf of Mexico and Lake Borgne area as water funneled into the narrow channels along many portions of the city (Shaffer et al. 2009). This caused many levees to fail, leading to devastating flooding in some of the most socially vulnerable city neighborhoods. Disaster recovery issues pertaining to Katrina's impacts on Louisiana and New Orleans have also been noted across many studies (e.g., Banipal 2006; Pyles 2011).

The inclusion of Katrina deaths within our analyses points to the importance of understanding how TC disasters can be complex and multi-layered events where characteristics of society and hazard intensity interact to result in significant loss to life. The Katrina-New Orleans, LA disaster also illustrates how a singular hazard event can overwhelm emergency management, leaving long-lasting consequences and issues for the communities affected. The trade-off is that extreme disaster events such as Katrina can skew trends and patterns in TC hazard fatalities, making it an outlier in terms of total fatalities and fatality causes compared to all other landfalling TCs during our study period. As such, we conducted our fatality analysis with and without Hurricane Katrina being considered (**Figure 1c-d**). Once removing direct

fatalities from Katrina, inland flooding became the majority (49% without Katrina) TC fatality cause instead of storm surge. Removing Katrina fatalities from the dataset also illustrates that TC winds (24% without Katrina) are more deadly than storm surge (17% without Katrina) on average. Overall, stratifying the proportion of TC deaths with and without considering Katrina provides greater insight into the TC hazards that are most likely to result in a fatality.

## 4.2 Tropical Cyclone Hazard Incidence

### 4.2.1 Inland Flash Flooding

As expected, TC hazard incidence is concentrated in the Gulf and Atlantic Coast regions (**Figure 2**). In terms of inland flash flooding incidence, two counties (Carteret and New Hanover, NC) have received over 14 cm of TCFF precipitation per year on average (mean). Again, TCFF precipitation grid cells are those 4-km QPE grid cells that exceed 5.8 cm (2 in) of precipitation in a 24-hr period. Six of the top 10 counties that rank highest in terms of TCFF occurrence are located in North Carolina (**Figure 2a; Table 1**). Many of these counties were strongly affected by the heavy rains from Hurricanes Florence (2018) and Helene (2024). Portions of Carteret and New Hanover, NC counties received more than 75 cm (~30 in) of precipitation over a five-day period from Hurricane Florence (NWS 2018). Other western North Carolina counties such as Polk County were most affected by Hurricane Helene, where over 40 cm (~15 in) of rain fell during a 24-hour timeframe (NHC 2024).

Of the top 100 ranked counties for TCFF precipitation or inland flooding potential, 33 are located in North Carolina, with 18 being in Louisiana and 17 in Florida. Also, 30 counties have experienced over 10 cm of TCFF precipitation from 2005 to 2024. When mapping the county-level percentile rankings for inland flooding incidence, coastal counties represent percentile

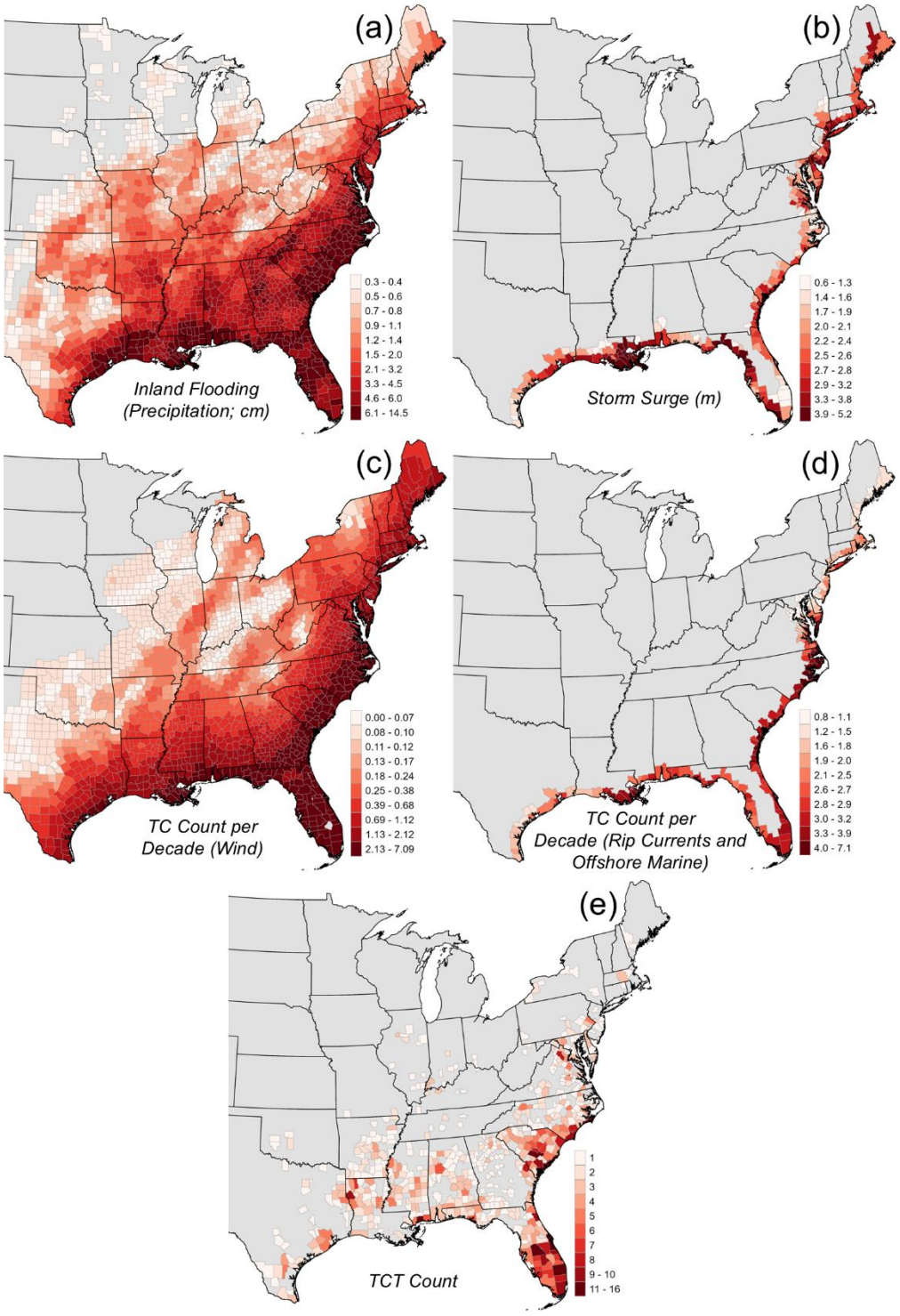


403

404 **Fig. 2** County TC hazard risk as determined by the (a) sum total amount of precipitation (cm)
405 from TCFF grid cells from 2005 to 2024, (b) mean storm surge height (m) for all landfalling TCs
406 across all TC intensity categories as estimated by the NOAA SLOSH model, total TC count and
407 associated TC wind incidence for (c) all CONUS counties and (d) coastal counties from 1851 to
408 2020, and (e) total TCT counts from 1995 to 2024.

**Table 1** County percentile rankings for TC hazard occurrence by hazard type.

| | Inland Flooding | | Storm Surge | | Wind | | Rip Current and Offshore Marine | | Tropical Cyclone Tornado (TCT) | |
|---|---|---|---|---|---|---|---|---|---|---|
| **Rank** | **State** | **County** | **State** | **County** | **State** | **County** | **State** | **County** | **State** | **County** |
| 1 | NC | Carteret | LA | St. Bernard | NC | Carteret | NC | Carteret | FL | Polk |
| 2 | NC | New Hanover | LA | Orleans | LA | St. Bernard | LA | St. Bernard | FL | Palm Beach |
| 3 | NC | Brunswick | LA | St. John Bap. | FL | Monroe | FL | Monroe | SC | Charleston |
| 4 | NC | Jones | LA | Plaquemines | NC | Dare | NC | Dare | SC | Orangeburg |
| 5 | NC | Pamlico | LA | St. Charles | NC | Pamlico | NC | Pamlico | MS | Harrison |
| 6 | MS | Harrison | FL | Citrus | NC | Tyrrell | NC | Tyrrell | SC | Beaufort |
| 7 | NC | Onslow | LA | St. James | NC | Hyde | NC | Hyde | FL | Brevard |
| 8 | TX | Orange | LA | Jefferson | NC | Currituck | NC | Currituck | FL | Indian River |
| 9 | LA | St. Charles | LA | Lafourche | LA | Plaquemines | LA | Plaquemines | LA | De Soto |
| 10 | MS | Hancock | FL | Hernando | SC | Beaufort | SC | Beaufort | NC | Brunswick |

rankings above the 93rd percentile. However, some inland counties located in central Georgia and western North Carolina are also within the 93rd percentile and greater for TCFF precipitation. Again, these were most affected by Hurricane Helene as the storm traversed inland, leading to catastrophic flooding near Asheville, NC and the Blue Ridge Mountains region of North Carolina (NHC 2024).

### 4.2.2 Storm Surge

All of the top 10 counties ranked in terms of storm surge incidence and severity are located in Florida and Louisiana (**Figure 2b; Table 1**). Two specific regions in Florida and Louisiana are at greatest risk of damaging storm surge, the Mississippi River delta region of Louisiana and the southern portion of Florida's Big Bend region. Citrus and Hernando counties just north of Tampa and Clearwater, FL are the two most storm surge-prone counties within Florida (**Figure 2**). Each of the top 10 counties with the greatest TC storm surge threat has a mean expected storm surge height from all hurricane intensities of 4.25 m and higher. St. Bernard and Orleans Parishes are the only two counties or parishes that have expected mean

storm surge height over 5 m, with St. Bernard Parish ranking highest with 5.2 m of expected storm surge from the average landfalling TC.

No Atlantic coastal counties are ranked in the top 20 for storm surge risk. However, Cumberland County, DE, Middlesex and Richmond, NJ Counties, and Putnam and Rockland, NY Counties are all within the 99$^{th}$ percentile for storm surge incidence and severity. This finding indicates that storm surge threats are not isolated to the Gulf of Mexico and southern portion of the Atlantic coastline. These counties are within the Delaware Bay region and Upper Bay, NY where the Hudson and East Rivers feed into the Atlantic Ocean. Several TCs within our dataset have led to damaging storm surge within the southern Louisiana, western Florida, Delaware Bay, and Upper Bay regions. Other TCs such as Debby (2024), Eta (2020), Helene (2024), Idalia (2023), and Nicole (2020) led to high storm surge along Florida's west coast. Lastly, Hurricanes Irene (2011) and Sandy (2012) resulted in flooding coastal areas surrounded by the Upper, Lower, Sandy Hook, Jamaica, and Raritan Bays surrounding many parts of the New York City Burroughs of Staten Island, Manhattan, and Queens. Together, these results indicate that storm surge can lead to deadly seawater inundation for many highly populated CONUS regions.

#### 4.2.3 Wind, Rip Currents, and Dangerous Offshore Marine Conditions

Similar to the rankings for TCFF precipitation or inland flooding, a majority of the counties ranked within the top 10 for TC wind risk are located in North Carolina. Six of the top 10 counties that are most threatened by TC winds are in North Carolina including: Carteret, Currituck, Dare, Hyde, Pamlico, and Tyrrell Counties (**Figure 2; Table 1**). St. Bernard Parish in Louisiana ranks second in terms of greatest TC wind risk, while Monroe County, FL, Plaquemines, LA, and Beaufort, SC comprise the remaining four positions within the top 10

447 counties for TC wind risk. Every county in Florida is within the 90$^{th}$ percentile and greater for
448 TC wind risk.

449 Because we use the NRI database for both TC wind and rip current/dangerous offshore
450 marine conditions, the top 10 county rankings for rip currents and offshore marine are identical
451 to the TC wind top 10 rankings. Three primary coastal regions stand out in terms of rip current
452 and dangerous offshore marine conditions: the Florida Keys, Mississippi Delta region of
453 Louisiana, and the Outer Banks area in North Carolina (**Figure 2d; Table 1**). In addition,
454 Beaufort County, SC is also ranked in the top 10 for TC rip current risk. Only St. Bernard and
455 Plaquemines Parishes in Louisiana are in both the top 10 rankings for storm surge and rip current
456 risk. Assessing larger scale geospatial patterns in rip current and dangerous offshore marine
457 county-level risk illustrates that the eastern Gulf Coast and southern Atlantic Coast from the
458 Outer Banks, NC regions, down to Miami Beach, Florida are most prone to rip current impacts.

459 **4.2.4 Tropical Cyclone Tornadoes**

460 Eastern and southern-central Florida, as well as eastern North and South Carolina have
461 witnessed the greatest number of TCTs since 2005 (**Figure 2e; Table 1**). Four of the top 10
462 counties when ranking them by the number of TCTs that have traversed the counties are located
463 in Florida (Polk, Palm Beach, Brevard, and Indian River). Polk and Palm Beach County, FL, as
464 well as Charleston County, SC have all experienced over 15 TCTs since 2005, with Polk County,
465 FL being impacted by 16 TCTs over the 20-year study period. While counties closer to the Gulf
466 and Atlantic coastlines are impacted more frequently by TCTs than those counties farther inland,
467 many inland counties contain a high historical incidence of TCTs. DeSoto Parish, LA and
468 Fauquier County, VA are both in the 99$^{th}$ percentile and greater for TCT hazard occurrence.

469 **4.3 Tropical Cyclone Hazard and Disaster Indices**

### 4.3.1 TC Hazard Risk ($TC_{HR}$)

TC hazard incidence, as measured by the $TC_{HR}$ index, is greatest for counties along the Gulf and Atlantic coastlines (**Figure 3**). When ranking counties by their $TC_{HR}$ scores, 10 of the top 25 are located in Louisiana parishes south of New Orleans, as well as coastal counties in Alabama and Mississippi. Several (12) coastal counties in South Carolina and North Carolina also rank within the top 25 for TC hazard risk. Many inland and landlocked counties are also within the 85$^{th}$ percentile and greater for all TC hazard risk. Specifically, counties in western Alabama, western Georgia, central Carolinas, and far western North Carolina near the Blue Ridge Mountains are all within the 85$^{th}$ percentile for TC hazard risk. Inland flooding is the TC hazard that is the primary driver for counties with elevated $TC_{HR}$ scores. For example, most counties in the Blue Ridge Mountain region are above the 90$^{th}$ percentile for inland flash flooding. The repetitive inland flooding impacts from landfalling TCs such as Cindy (2005), Florence (2018), Fred (2021), Michael (2018), Zeta (2020), etc. over the last 20 years have led to this region experiencing several flash flooding events. Most notably, Hurricane Helene in 2024 devastated the region, producing over 50 cm (20 inches) in some western North Carolina regions. The difference between inland and coastal counties in terms of $TC_{HR}$ scores is that most coastal counties are not only ranked high for inland flash flooding but also ranked high for other TC hazards such as storm surge, wind and rip currents. However, inland counties do not experience storm surge or rip currents, so their $TC_{HR}$ score rankings are generally lower.

Four of the top 10 counties that have the greatest risk for TC hazards are located in North Carolina (Brunswick, Carteret, New Hanover, and Pamlico; **Table 2**). The top three counties in the CONUS in terms of $TC_{HR}$ scores are in North Carolina, with Carteret County being ranked highest of all CONUS counties. Carteret County, NC is the highest (100$^{th}$ percentile) ranked

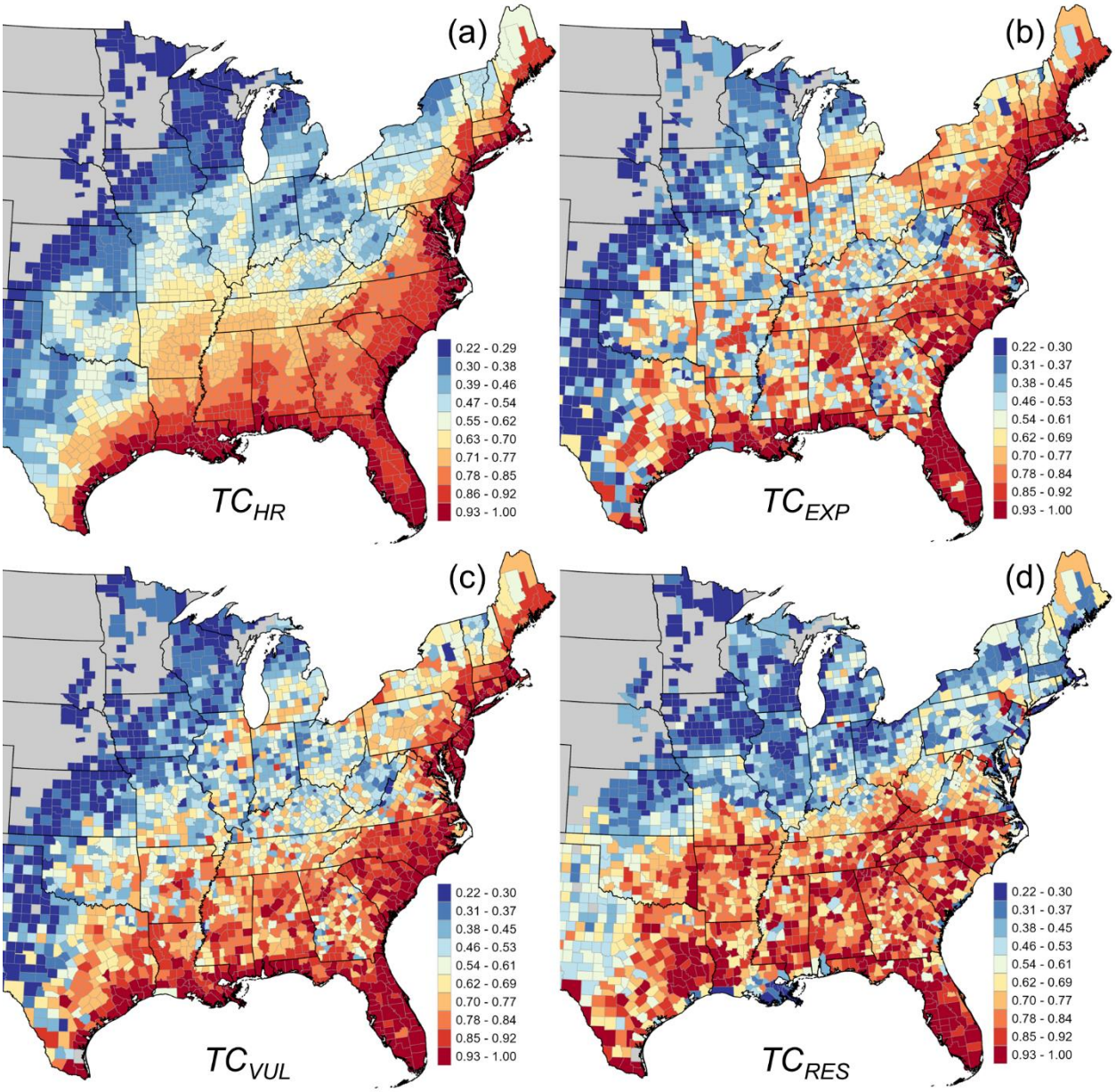


**Fig. 3** County percentile rankings for TCDR index components: (a) $TC_{HR}$, (b) $TC_{EXP}$, (c) $TC_{VUL}$, and (d) $TC_{RES}$.

**Table 2** TC hazard-prone county percentile rankings for $TC_{HR}$, $TC_{EXP}$, $TC_{VUL}$, and $TC_{RES}$ indices.

| | $TC_{HR}$ | | $TC_{EXP}$ | | $TC_{VUL}$ | | $TC_{RES}$ | |
|---|---|---|---|---|---|---|---|---|
| **Rank** | **State** | **County** | **State** | **County** | **State** | **County** | **State** | **County** |
| 1 | NC | Carteret | FL | Pinellas | TX | Harris | NY | Bronx |
| 2 | NC | Brunswick | FL | Hillsborough | FL | Miami-Dade | TX | Hidalgo |
| 3 | NC | New Hanover | FL | Duval | FL | Duval | FL | Citrus |
| 4 | MS | Jackson | TX | Harris | FL | Hillsborough | FL | Hendry |
| 5 | LA | Jefferson | FL | Miami-Dade | MS | Harrison | FL | Lee |
| 6 | NC | Pamlico | FL | Broward | AL | Mobile | TX | Cameron |
| 7 | LA | Lafourche | FL | Pasco | FL | Broward | FL | Sarasota |
| 8 | FL | Franklin | LA | Jefferson | LA | Jefferson | NY | Kings |
| 9 | FL | Pinellas | FL | Brevard | FL | Palm Beach | FL | Hernando |
| 10 | MS | Harrison | AL | Mobile | FL | Pinellas | FL | DeSoto |

county for inland flash flooding incidence, rip currents, dangerous offshore marine conditions, and TC winds. Carteret County is also ranked in the 99$^{th}$ percentile for TCT occurrence and in the 96$^{th}$ percentile for storm surge risk. The high TC hazard incidence for Carteret County, NC is expected given its location in the Outer Banks region of the state. Although Brunswick (Wilmington, NC) and New Hanover, NC Counties are not directly a part of the Outer Banks region of North Carolina, they also rank high for overall TC hazard risk. The remaining seven counties in the top 10 for $TC_{HR}$ scores share high percentile rankings (90$^{th}$ percentile and greater) for each individual TC hazard. All these counties are in the 99$^{th}$ percentile and greater for inland flooding, and in the 95$^{th}$ and greater percentile for storm surge, wind, rip currents, and dangerous offshore marine conditions.

### 4.4.2 TC Hazard Exposure ($TC_{EXP}$)

The $TC_{EXP}$ index calculation brings together both historical TC hazard incidence (i.e., TC hazard risk) and total population (**Figure 3b**; **Figure 4a-b**) to determine the counties where a large number of people may be subject to TC hazards and disaster impacts. All but three counties ranked in the top 10 for TC hazard exposure are located in Florida (**Table 2**). This finding, along

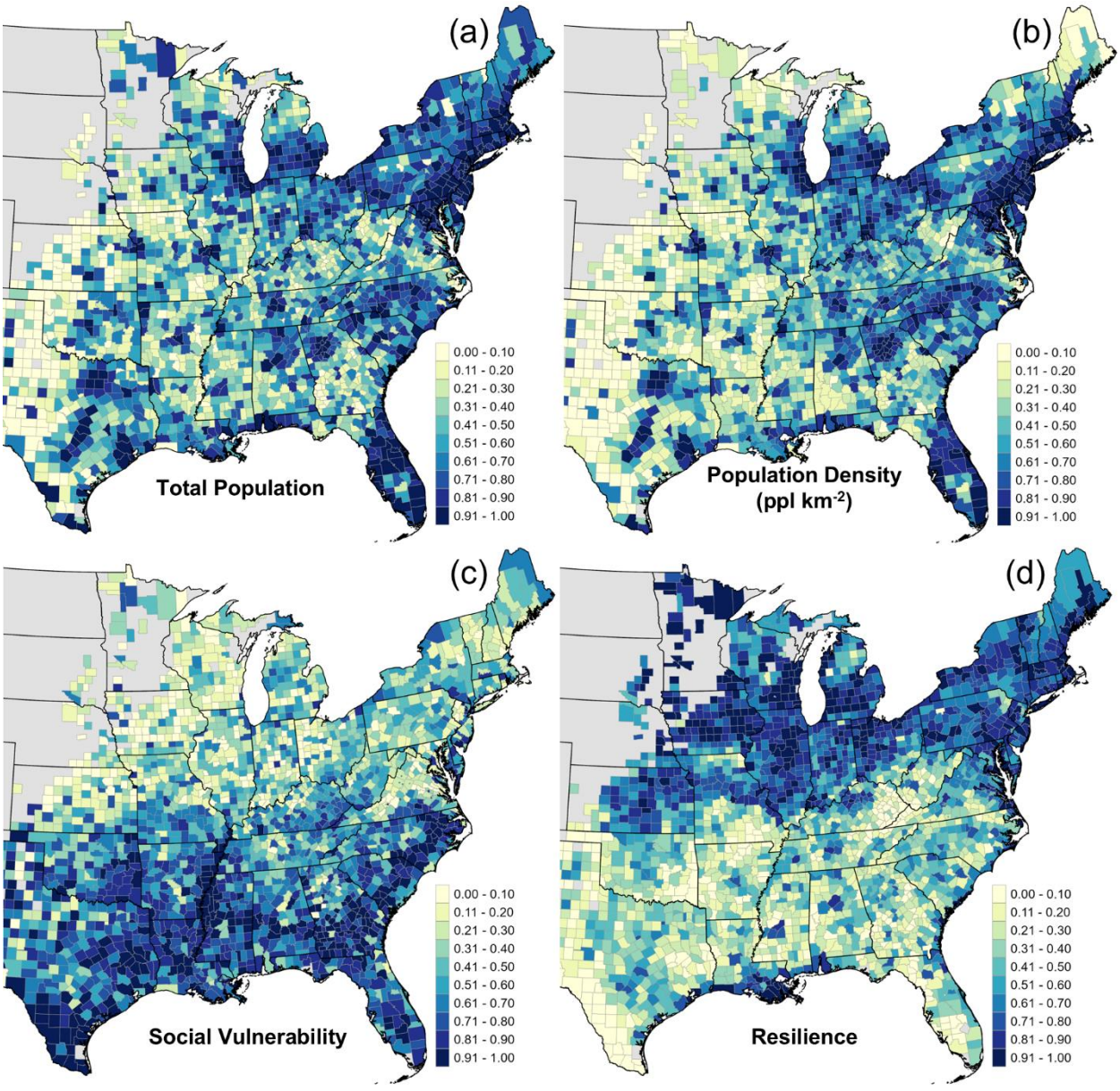


**Fig. 4** County (a) total population and (b) population density based on 5-year (2018-2023) ACS estimates. Panel (c) illustrates county overall 2022 CDC SVI percentile rankings. Panel (d) indicates county 2020 NRI overall resilience percentile rankings.

with the $TC_{HR}$ index scores, indicates that not only do Florida counties experience greater than average TC hazard frequency, the state's high population density also means exposure to TC hazards is higher than any other region in the CONUS. Florida counties with elevated $TC_{EXP}$ score rankings are located in three primary regions of the state: Tampa Bay to the Port Charlotte

526 and Cape Coral coastal region, West Palm beach to Miami-Dade County coastal region, and
527 Palm Bay to Jacksonville along Florida's Atlantic Coast.

528 Other counties ranked high for $TC_{EXP}$ are located in clusters across several states or
529 regions. For instance, Brazoria, Harris, and Galveston, TX Counties are all ranked in the top 25
530 for $TC_{EXP}$. High $TC_{EXP}$ rankings ($90^{th}$ percentile and greater) for these counties are a result of the
531 built-environment and developed land sprawl associated with the Houston, TX metropolitan area
532 over the last 80 years being collocated with high TC hazard incidence. The combination of
533 sprawling metropolitan areas and high hazard incidence is also evident in many other counties
534 within the top 25 for $TC_{EXP}$. Counties such as Jefferson and St. Tammany Parishes in Louisiana,
535 Baldwin and Mobile Counties in Mississippi and Alabama, and many North and South Carolina
536 counties associated with cities such as Charleson, SC, Myrtle Beach, SC, and Wilmington, NC
537 all have large population density and high TC hazard occurrence that leads to greater odds of TC
538 hazard impacts.

539 Using bivariate maps between county TC hazard risk and population exposure (**Figure**
540 **5a**), the spatial relationship between these two disaster variables becomes more apparent. For
541 instance, nearly all Florida counties are within the $90^{th}$ percentile and greater for TC hazard
542 exposure and rank in the high hazard risk and high exposure bivariate category. Counties as far
543 north as southeastern Michigan, northeastern Ohio, and southwestern New York all indicate high
544 hazard risk and exposure. Other highly populated metropolitan areas and counties that also fall
545 within the $90^{th}$ percentile and greater for TC exposure and indicate having high risk and high
546 exposure are Birmingham, AL, Little Rock, AR, Atlanta, GA, Charlotte, NC, Philadelphia, PA,
547 New York City, NY, Memphis, TN, and Houston, TX. The counties farthest away from the Gulf
548 or Atlantic coastlines that are within the 90th percentile and greater for TC hazard exposure are

549 Jefferson County, AL (Birmingham, AL), Tuscaloosa County, AL (Tuscaloosa, AL), and Pulaski
550 County, AR (Little Rock, AR).

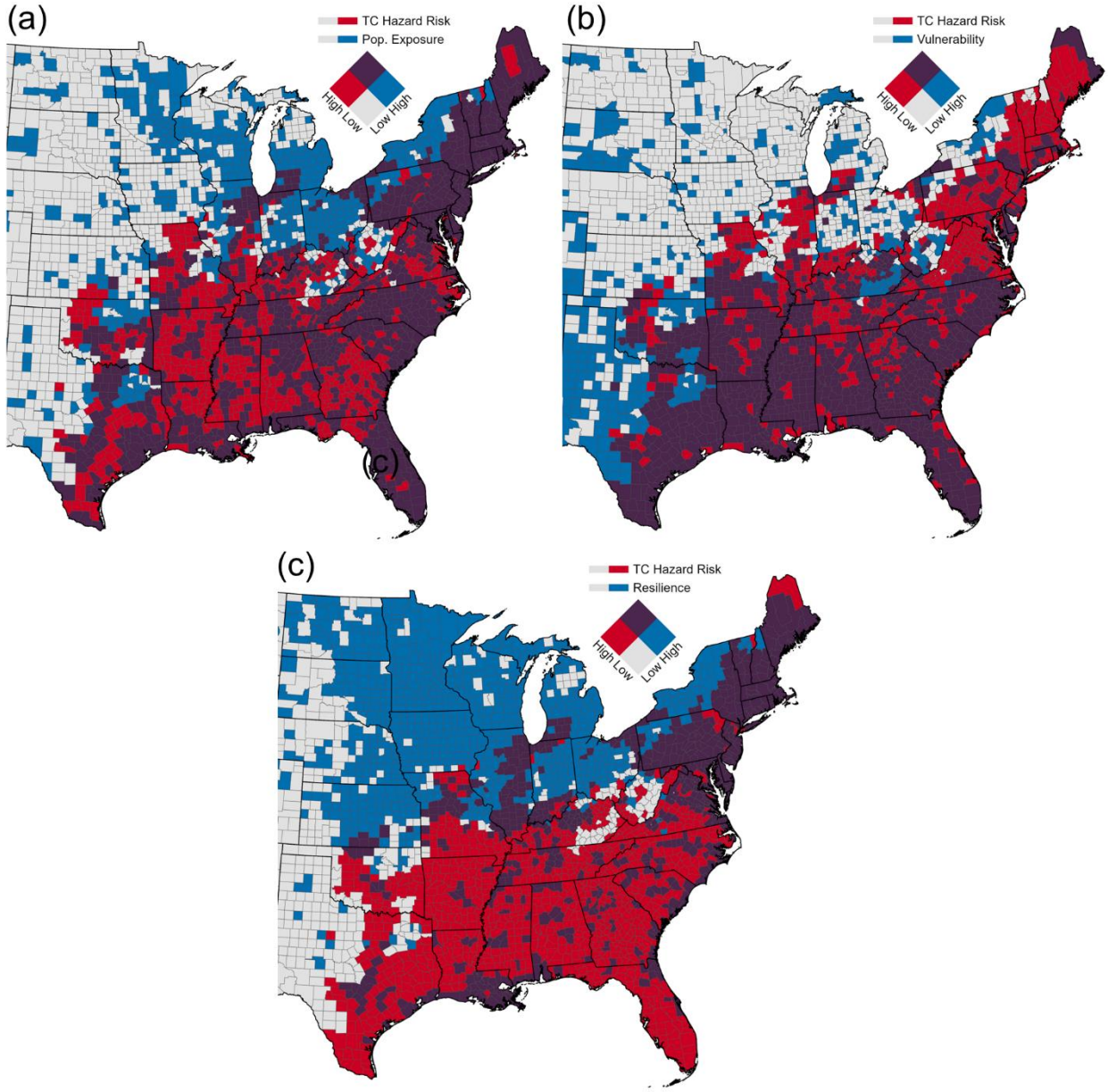


551

552 **Fig. 5** Bivariate maps of all TC hazard risk against (a) total population exposure, (b) social
553 vulnerability, and (c) disaster resilience.

554

555 counties within the 90$^{th}$ percentile and greater for TC hazard exposure that are farthest away
556 from the Gulf or Atlantic Coasts. This result, in combination with the $TC_{HR}$ index scores, again

suggests that although many inland counties experience fewer TC hazards than coastal counties, the high population density associated with many inland metropolitan areas can lead to significant impacts. All of these findings confirm prior research that has illustrated that population and development growth is a strong control for hazard impact severity and frequency (e.g., Freeman and Ashley 2017; Fussell et al. 2017).

### 4.2.3 TC Vulnerability ($TC_{VUL}$)

$TC_{VUL}$ scores indicate that many Alabama, Florida, Louisiana, Mississippi, South Carolina, and Texas coastal counties are highly vulnerable to TC hazards (**Figure 3c, 4c, 5b)**. Six of the top 10 county rankings for $TC_{VUL}$ scores are in Florida, with Miami-Dade, Duval, and Hillsborough Counties being ranked second, third, and fourth for TC hazard vulnerability (**Table 2**). However, Harris County, TX (Houston) is ranked highest of all CONUS counties for TC hazard vulnerability. Harris County's high $TC_{VUL}$ score is mostly driven by high SVI measures for housing cost burden (96$^{th}$ percentile), no health insurance (97$^{th}$ percentile), aged 17 and younger (92$^{nd}$ percentile), language barriers (98$^{th}$ percentile), minority populations (97$^{th}$ percentile), multi-unit structures (99$^{th}$ percentile), and crowding (96$^{th}$ percentile). Together, these variables suggest that Harris County is highly vulnerable due to socioeconomic status (SVI Theme 1) and racial and ethnic minority status (SVI Theme 3) constituents.

Florida counties within the top 10 for $TC_{VUL}$ scores follow similar trends to each other given all six counties are above the 95$^{th}$ percentile for SVI housing cost burden, 80$^{th}$ percentile for language barriers, and 96$^{th}$ percentile for multi-unit structures. The remaining top 10 $TC_{VUL}$ county score rankings include Harrison County, MS (Ranked 5$^{th}$), Jefferson Parish, LA (Ranked 8$^{th}$), and Mobile County, AL (Ranked 6$^{th}$). For Harrison County, high SVI metrics include unemployment (92$^{nd}$ percentile), housing cost burden (93$^{rd}$ percentile), and single parent head of

household (94th percentile). These findings suggest that socioeconomic status and household characteristics are critical for creating vulnerability in Harrison County. Jefferson Parish, LA is similar to Harrison County, MS given its high housing cost burden (94th percentile); but other vulnerability factors such as language barriers (92nd percentile), multi-unit structures (93rd percentile), and minority populations (87th percentile) are much higher than both Harrison County and median SVI scores (i.e., 50th percentile). For Mobile County, AL, there is no single SVI measure that stands out in terms of overall social vulnerability, but the county does have elevated (greater than 85th percentile) measures for housing burden cost (89th percentile). In general, coupling these high-vulnerability characteristics with a high incidence of TC hazards points to these counties being most likely to experience and suffer from a TC disaster.

Examining the top 25 rankings for $TC_{VUL}$ also reveals that counties such as Cameron, TX, Horry, SC, and Prince George's, MD also contain greater TC hazard vulnerability than most other TC hazard-prone counties. All top 25 ranked $TC_{VUL}$ counties share similar vulnerability characteristics to each other regarding high housing cost burden, language barriers, and minority populations. Inland counties associated with large metropolitan areas such as Dallas, TX, Little Rock, AR, Birmingham, AL, Atlanta, GA, and San Antonio, TX are also within the 90th percentile and greater for $TC_{VUL}$ scores. Again, these counties all share vulnerability measures higher (80th percentile and greater) than the median CONUS county for housing cost burden, language barriers, minority populations, and multi-unit structures. Davidson County, TN (Nashville, TN) is the farthest county from the Atlantic or Gulf coastlines that is ranked in the 90th percentile and greater for TC hazard vulnerability. The coastal Maine counties of Cumberland (91st percentile) and Washington (92nd percentile) are the counties that are farthest

602 north in the CONUS that are still within the 90$^{th}$ percentile and greater for TC hazard
603 vulnerability.

604 Lastly, the bivariate maps in **Figure (5b)** indicate that much of the rural southeastern
605 CONUS, including eastern Texas, eastern Oklahoma, and Southern Missouri all have high
606 hazard risk the coincides with high social vulnerability. However, some counties located in the
607 Northeast, Great Lakes, and Midwest regions also indicate high risk juxtaposed with high
608 vulnerability. Together, these findings suggest that non-coastal counties far away from the
609 location of TC landfall are also prone to TC disasters because of elevated inland flooding and
610 wind risk coupled with vulnerability populations.

611 **4.2.4 TC Resilience ($TC_{RES}$)**

612 When combining total population and TC hazard incidence through our $TC_{RES}$ index,
613 Bronx County, NY is identified as the TC-hazard prone county with the lowest TC disaster
614 resilience (**Figures 3d, 4d, 5c**). Kings County, NY is also ranked within the top 10 for $TC_{RES}$
615 scores because of its high population density, TC hazard incidence, and having low resilience
616 (**Table 2**). Although higher percentile rankings for $TC_{RES}$ indicate lower county resilience (i.e.,
617 $TC_{RES}$ is calculated as one minus the resilience percentile ranking), BRIC estimates are the
618 opposite. Lower BRIC percentile rankings for counties indicate worse overall community
619 resilience to disasters (See **Eq. 4**). Kings County ranks below the 6$^{th}$ percentile for social,
620 community, and environmental BRIC categories. Bronx County ranks in the 1$^{st}$ percentile for
621 social, 16$^{th}$ percentile for economic, 1$^{st}$ percentile for community, and 2$^{nd}$ percentile for
622 environmental resilience to disasters based on the BRIC dataset. These low BRIC mean that
623 Bronx County has extremely low disaster resilience compared to all other CONUS counties.

Taking all BRIC category scores and percentile rankings into account, Bronx County is within the 6$^{th}$ percentile for overall resilience.

The remaining top 10 counties for lowest TC disaster resilience are in Florida or Texas. Specifically, six of the 10 counties with the lowest disaster resilience as calculated by $TC_{RES}$ are in Florida, including Citrus, Hendry, Lee, Sarasota, Hernando, and DeSoto Counties. Each of these counties ranks below the 10$^{th}$ percentile for overall resilience scores. Citrus, DeSoto, and Hendry Counties are all below the 20$^{th}$ percentile for social, infrastructure, and community resilience categories, with Hernando, Lee, and Sarasota Counties having low (less than the 10$^{th}$ percentile) resilience in terms of environmental and community BRIC categories. Hidalgo and Cameron Counties in Texas comprise the remaining top 10 $TC_{RES}$ rankings, with both of the counties having very low resilience in terms of social (1$^{st}$ percentile BRIC score) and community (6$^{th}$ percentile BRIC score).

From a spatial distribution standpoint, counties with low TC disaster resilience as indicated by $TC_{RES}$, are dispersed throughout the CONUS, with many inland counties within eastern Oklahoma, southern Missouri, western Kentucky, and those throughout the southern Appalachian Mounties region being within the 90$^{th}$ percentile and greater for $TC_{RES}$ scores. In fact, several counties farther west in Arizona (Conchise), New Mexico (Dona Aña and Otero), and Texas (El Paso) are also in the 90$^{th}$ percentile and greater for $TC_{RES}$ score rankings. The common traits these counties share are their low community and environmental resilience (20$^{th}$ percentile and greater BRIC scores). The counties that are farthest north that still rank within the 90$^{th}$ percentile and greater for $TC_{RES}$ are in far northeastern Pennsylvania (i.e., Monroe (96$^{th}$ percentile), Pike (97$^{th}$ percentile), and Wayne (90$^{th}$ percentile)).

Again, most southeastern CONUS counties fall into the high TC hazard risk and low community resilience category (**Figure 5c**). Southern Louisiana counties indicate high risk coupled with high resilience. This is most likely attributed to FEMA's Building Resilient Infrastructure and Communities program, which many opted into, that provided resources aimed at building resilience (Association of State Floodplain Managers 2025). This program was specifically aimed at helping residents raise their homes above flood levels, build levees, and prevent flooding. However, the program ended in Spring 2025, leaving these residents less resilient as indicated in our county-level analysis. Unfortunately, we are unable to adjust our analysis to account for this change. As such, it is expected that many of these high risk-high resilience counties in Louisiana are actually high risk-low resilience. Nevertheless, most high risk-low resilience counties are associated with rural regions outside of major cities such as Atlanta, GA, Houston, TX, Little Rock, AR, and Birmingham, AL. Many low risk-high resilience counties are in the upper Midwest in states such as Iowa, Minnesota, and Wisconsin. This is attributed to their relatively low TC hazard occurrence and overall low vulnerability.

#### 4.2.5 TC Disaster Risk (TCDR)

The TCDR index brings components of hazard incidence, exposure, vulnerability, resilience, and fatalities together to estimate disaster likelihood when TCs threaten the CONUS. The spatial patterns in TCDR scores and rankings indicate that CONUS regions such as Florida, the Alabama, Louisiana, Mississippi, and Texas coastlines, North and South Carolina, as well as northeastern CONUS where highly populated cities such as Baltimore, Boston, New York City, Philadelphia, and Washington D.C. are located tend to have high TCDR scores (**Figure 6**). This result was expected given the proximity of these regions to the Gulf of Mexico and Atlantic Ocean where TC hazard risk is high. However, several inland regions or counties are also ranked

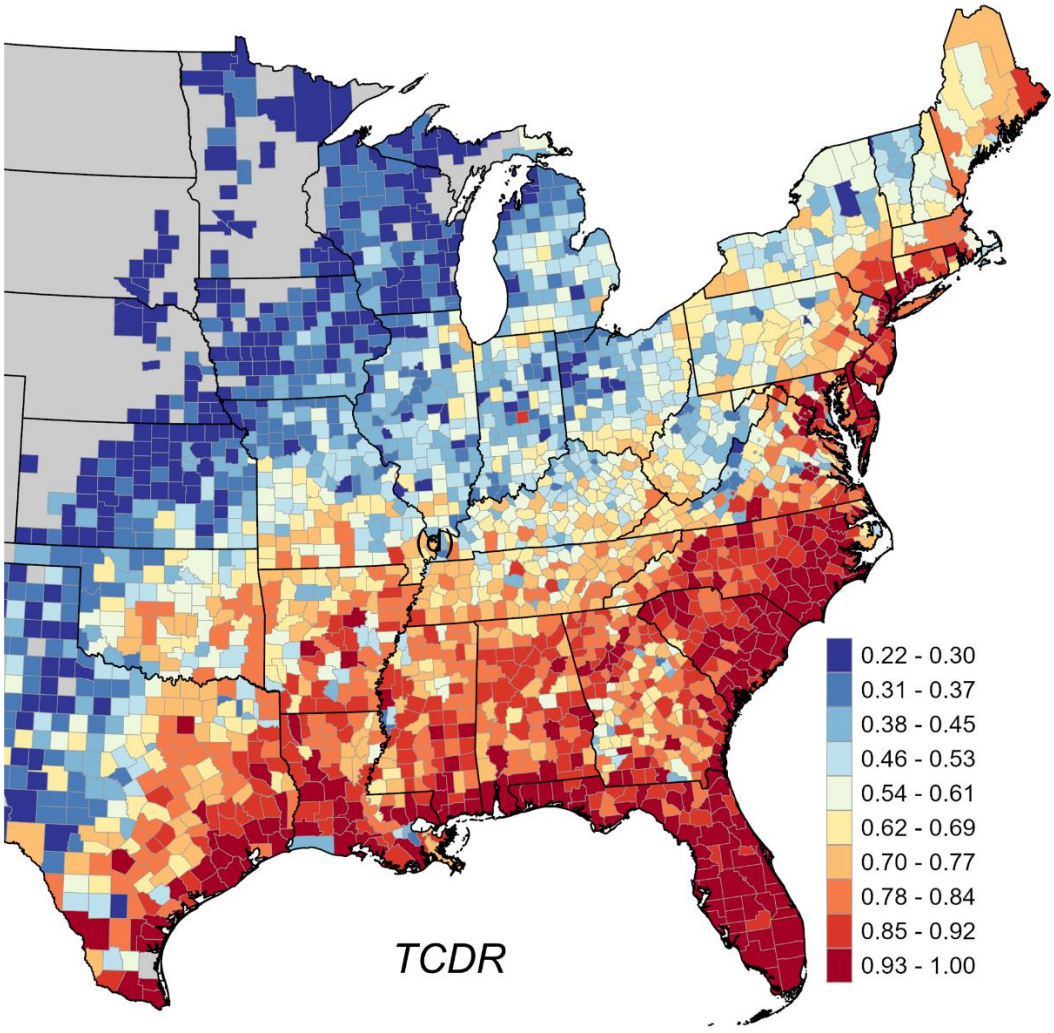


669

670 **Fig. 6** County percentile rankings for TCDR index calculations.

671

672 high in terms of their TCDR scores. For instance, White County, AR is more than 500 km from
673 the nearest coastline and is ranked in the 93rd percentile for TCDR scores due to its elevated
674 exposure ($TC_{EXP}$ 87th percentile), high vulnerability ($TC_{VUL}$ 90th percentile), and low resilience
675 ($TC_{RES}$ 93rd percentile). Although exposure, vulnerability, and resilience are strong controls for
676 many high inland county TCDR scores, these counties can also be subject to high TC hazard
677 risk. Again, as an example, White County, AR is ranked in the 82nd percentile for both inland
678 flooding and TCT risk. Other inland counties across the CONUS that are also highly TC disaster

679 prone include Butler County, MO, Davison County, TN, Warren County, TN, Pulaski County,
680 AR, and Marion County, IN. Each of these inland counties ranks above the 85$^{th}$ percentile for
681 TCDR, with the primary drivers of their elevated TCDR index rankings being inland flooding
682 risk coupled with high exposure, high vulnerability, and low resilience.

683 Although our results indicate that many inland counties have high TC disaster potential,
684 TC disaster likelihood is ultimately greatest along the coastal regions on the CONUS. Six of the
685 top 10 counties with the highest TCDR scores are located in Florida, with coastal Texas and New
686 York counties making up the remaining four spots in the top 10 TCDR index rankings (**Table 3**).
687 Harris County, TX is considered the most TC disaster-prone county in the CONUS based on our
688 TCDR analysis. Harris County ranks in the 96$^{th}$ percentile for both $TC_{HR}$ and $TC_{EXP}$ metrics, as
689 well as in the 80$^{th}$ percentile for $TC_{VUL}$ and 87$^{th}$ percentile for $TC_{RES}$. Although Harris County is
690 not ranked in the top 10 for any TC hazard incidence, its high population density, high social
691 vulnerability, and low resilience suggest that when a TC does impact the county, the
692 consequences of the TC hazards may result in a disaster. Hurricane Harvey (2017) is a prime
693 example of how a landfalling TC can have devastating consequences on Harris County. Cameron
694 County, TX is ranked second of all counties for TCDR index scores. Similar to Harris County,
695 Cameron County has elevated TC hazard incidence for inland flooding (81$^{st}$ percentile), storm
696 surge (93$^{rd}$ percentile), wind (90$^{th}$ percentile), rip currents and dangerous offshore marine
697 conditions (96$^{th}$ percentile), and TCTs (94$^{th}$ percentile).

698 Pinellas and Lee Counties in Florida are ranked third and fourth for TCDR index scores,
699 making them the most TC disaster-prone counties in Florida. These two counties rank above the
700 92$^{nd}$ percentile for all TC hazards and in the 99$^{th}$ percentile for $TC_{EXP}$, $TC_{VUL}$, and $TC_{RES}$ scores.
701 When considering the top 25 county TCDR rankings, 18 counties are located in Florida. Nearly

**Table 3** TC hazard-prone county percentile rankings for the TCDR index.

| Rank | State | County |
|---|---|---|
| 1 | TX | Harris |
| 2 | TX | Cameron |
| 3 | FL | Pinellas |
| 4 | FL | Lee |
| 5 | FL | Pasco |
| 6 | FL | Palm Beach |
| 7 | FL | Miami-Dade |
| 8 | NY | Bronx |
| 9 | NY | Queens |
| 10 | FL | Hillsborough |
| 11 | FL | Hernando |
| 12 | FL | Manatee |
| 13 | NY | Kings |
| 14 | FL | Collier |
| 15 | FL | Broward |
| 16 | FL | Charlotte |
| 17 | FL | Citrus |
| 18 | FL | Escambia |
| 19 | FL | Bay |
| 20 | FL | St. Lucie |
| 21 | FL | Volusia |
| 22 | MD | Prince George's |
| 23 | NJ | Essex |
| 24 | FL | Monroe |
| 25 | FL | Sarasota |

all of these Florida counties have combined high TC hazard incidence juxtaposed with elevated measures of exposure and vulnerability. Other top 25 TCDR ranked counties are Bronx, Kings, and Queens Counties in New York, Prince George's County in Maryland, and Essex County in New Jersey. Bronx and Queens, NY counties are the highest TCDR-ranked counties not located in Texas or Florida. Their higher TCDR rankings are attributed to large population exposure combined with high vulnerability. The same holds true for Kings County, NY and Prince George's, MD counties.

## 5 Conclusions

This study examined the relationships between TC hazard incidence, population exposure, societal vulnerability, and community resilience through a geospatial lens to provide a baseline understanding of county-level TC disaster potential across the CONUS. We assessed

714 these relationships through the creation of indices that determine the counties that are most likely
715 to be impacted by TC hazards and suffer from a disaster. A list of conclusions is provided below:

716 • TC disaster potential, frequency, and severity is, at a minimum, a function of hazard
717 incidence, exposure, vulnerability, and resilience. Counties where frequent TC hazard
718 incidence overlaps with large population exposure, high vulnerability, and low
719 resilience are more prone to hazard impacts and disasters.

720 • Inland flooding is responsible for nearly half of all historical direct fatalities from
721 TCs when considering Hurricane Katrina's storm surge deaths as an outlier.
722 Conversely, the large number of people killed by Hurricane Katrina's storm surge
723 indicates that a singular TC event that traverses an area of high exposure and
724 vulnerability can lead to a high-fatality disaster, regardless of historical trends in
725 disaster incidence and fatalities by hazard type.

726 • Counties in North Carolina are most likely to experience inland flooding, severe
727 wind, dangerous offshore marine conditions and rip currents. Counties in Louisiana
728 are most likely to experience storm surge, while Florida counties are expected to
729 witness the greatest number of TCTs. When considering all TC hazards, TC hazard
730 incidence is generally higher for counties in Florida, Louisiana, and North Carolina.

731 • Our TC disaster indices suggest that counties in Florida, Louisiana, North Carolina,
732 and southeastern Texas rank well above the CONUS median in terms of TC exposure,
733 vulnerability, and low resilience. Yet, some highly populated metropolitan areas such
734 as Houston, TX and New York City, NY are also disaster prone due to their high
735 population density and social vulnerability.

- Harris County, TX (Houston, TX), Cameron County, TX, Pinellas County, FL, and Lee County, FL are the most disaster-prone (>99$^{th}$ percentile) counties in the CONUS based on our analysis.

County, State, and Federal emergency managers should use these findings as a baseline understanding for expected TC hazard impacts on their communities. Policymakers and stakeholders should develop new and/or alter existing resilience-building strategies so that their efforts are aimed at reducing impacts on the vulnerable populations that are most likely to suffer and/or be killed during a TC event. By not treating all TC hazards equally across the CONUS in terms of their fatality-producing likelihood, new and targeted mitigation actions and strategies can be developed so that hazard impacts and disaster losses are reduced. Policies and standards have been altered after a high-impact TC event in the past. For example, following Hurricane Andrew in 1992, the U.S. Department of Housing and Urban Development (HUD) changed construction standards for manufactured homes in coastal regions so that they were more wind resistant (Rumbach 2020). Similar mitigation actions were taken after Hurricane Katrina with the development of the Lake Borgne surge barrier that is designed to protect New Orleans from future TCs that may cause significant storm surge (Huntsman 2011). Overall, these examples are evidence that post-event mitigation actions are critical to preventing future disasters, but results from this work should be applied in a proactive manner prior to the next TC event. Doing such will reduce losses in the future, while also providing economic and social opportunities for many TC hazard-prone counties.

This work and our findings are not presented without limitations. Outcomes from this research are spatially coarse. Our methods and analyses were limited by data input resolution and temporal availability. For instance, the QPE data employed in this study is not available prior to

2005, limiting our ability to examine TC precipitation for years prior. Other limitations were apparent because of the spatial resolution of the datasets we used within the exposure, vulnerability, and resilience analyses. CDC SVI data is only available at the Census tract and county scale, whereas NRI resilience estimates are only made available for county enumerations. Future research should concentrate efforts on singular TC hazards and for counties where TC disaster potential is elevated (i.e., 95$^{th}$ percentile and greater TCDR scores). Doing such will allow researchers to provide community-specific recommendations that are aimed at TC hazards that are most likely to affect local populations.

**Acknowledgements**

We would like to thank the NOAA and NHC forecasters and researchers for their efforts in compiling historical reports and data on tropical cyclone events.

**Author contributions**

All authors contributed to the analysis and research design. S.M.S.was responsible for idea formation, a majority of data analysis, research execution, methodology, figure creation, manuscript writing and formatting. S.J.W. and T.M.L. are responsible for a portion of the precipitation and TC climatology portion of the research. C.M.C. is responsible for a portion of the TCT analysis. All authors participated in manuscript proofreading, formatting, and presentation.

**Data availability**

All data employed and analyzed in this study is publicly available.

**Declarations**

The authors have no relevant financial or non-financial interests to disclose.

## References

American Society of Civil Engineers (ASCE) (2025) FEMA ends Building Resilient Infrastructure and Communities Program. Infrastructure Report Card. Accessed 28 May 2025. https://infrastructurereportcard.org/fema-ends-bric-program/

Anderson GB, Ferreri J, Al-Hamdan M, Crosson W, Schumacher A, Guikema S, Quiring S, Eddelbuettel D, Yan M, Peng RD (2020) Assessing United States county-level exposure for research on tropical cyclones and human health. Environ Health Perspect 128(10):107009. https://doi.org/10.1289/EHP6976

Atallah E, Bosart LF, Aiyyer AR (2007) Precipitation distribution associated with landfalling tropical cyclones over the eastern United States. Mon Weather Rev 135(6):2185–2206. https://doi.org/10.1175/MWR3382.1

Banipal K (2006) Strategic approach to disaster management: lessons learned from Hurricane Katrina. Disaster Prev Manag 15(3):484–494. https://doi.org/10.1108/09653560610669945

Bjarnadottir S, Li Y, Stewart MG (2011) Social vulnerability index for coastal communities at risk to hurricane hazard and a changing climate. Nat Hazards 59(2):1055–1075. https://doi.org/10.1007/s11069-011-9817-5

Bobby SA (2012) Disaster risk index (DRI) for tropical cyclone of Bangladesh. Int J Eng Res Technol 1(3):1–6

Booth JF, Narinesingh V, Towey KL, Jeyaratnam J (2021) Storm surge, blocking, and cyclones: A compound hazards analysis for the northeast United States. J Appl Meteorol Climatol 60(11):1531–1544. https://doi.org/10.1175/JAMC-D-21-0062.1

804 Boyd EC (2010) Estimating and mapping the direct flood fatality rate for flooding in greater
805 New Orleans due to Hurricane Katrina. Risk Hazards Crisis Public Policy 1(3):91–114.
806 https://doi.org/10.2202/1944-4079.1017
807 Cui W, Caracoglia L (2016) Exploring hurricane wind speed along US Atlantic coast in warming
808 climate and effects on predictions of structural damage and intervention costs. Eng Struct
809 122:209–225. https://doi.org/10.1016/j.engstruct.2016.05.003
810 Cutter SL, Burton CG, Emrich CT (2010) Disaster resilience indicators for benchmarking
811 baseline conditions. J Homeland Secur Emerg Manage 7(1):1–24.
812 https://doi.org/10.2202/1547-7355.1732
813 Cutter SL (2024) The origin and diffusion of the social vulnerability index (SoVI). Int J Disaster
814 Risk Reduct 109:104576. https://doi.org/10.1016/j.ijdrr.2024.104576
815 Cutter SL, Ash KD, Emrich CT (2014) The geographies of community disaster resilience. Glob
816 Environ Change 29:65–77. https://doi.org/10.1016/j.gloenvcha.2014.08.005
817 Cutter SL, Gall M (2006) Hurricane Katrina: A failure of planning or a planned failure.
818 Naturrisiken und Sozialkatastrophen. Available online at
819 https://www.researchgate.net/profile/Melanie-
820 Gall/publication/253398380_Chapter_27_Hurricane_Katrina_A_Failure_of_Planning_or
821 _a_Planned_Failure/links/0a85e53b4494c24ac5000000/Chapter-27-Hurricane-Katrina-
822 A-Failure-of-Planning-or-a-Planned-Failure.pdf
823 Davidson RA, Lambert KB (2001) Comparing the hurricane disaster risk of US coastal counties.
824 Nat Hazards Rev 2(3):132–142. https://doi.org/10.1061/(ASCE)1527-
825 6988(2001)2:3(132)

826 Do C, Kuleshov Y (2023) Tropical cyclone multi-hazard risk mapping for Queensland,
827 Australia. Nat Hazards 116(3):3725–3746. https://doi.org/10.5194/nhess-2022-139
828 Edwards R (2012) Tropical cyclone tornadoes: A review of knowledge in research and
829 prediction. E-Journal Severe Storms Meteorol 7(6):1–61.
830 https://doi.org/10.55599/ejssm.v7i6.42
831 FEMA (2023) National Risk Index. Federal Emergency Management Agency, Washington, D.C.
832 https://hazards.fema.gov/nri/data-resources
833 Flanagan BE, Gregory EW, Hallisey EJ, Heitgerd JL, Lewis B (2011) A social vulnerability
834 index for disaster management. J Homeland Secur Emerg Manage 8(1):1-24.
835 https://doi.org/10.2202/1547-7355.1792
836 Freeman AC, Ashley WS (2017) Changes in the US hurricane disaster landscape: the
837 relationship between risk and exposure. Nat Hazards 88(2):659–682.
838 https://doi.org/10.1007/s11069-017-2885-4
839 Fussell E, Curran SR, Dunbar MD, Babb MA, Thompson L, Meijer-Irons J (2017) Weather-
840 related hazards and population change: A study of hurricanes and tropical storms in the
841 United States, 1980–2012. Ann Am Acad Polit Soc Sci 669(1):146–167.
842 https://doi.org/10.1177/0002716216682942
843 Gensini VA, Ashley WS (2010) An examination of rip current fatalities in the United States. Nat
844 Hazards 54(1):159–175. https://doi.org/10.1007/s11069-009-9458-0
845 Gentry RC (1983) Genesis of tornadoes associated with hurricanes. Mon Weather Rev
846 111(9):1793–1805. https://doi.org/10.1175/1520-0493(1983)111
847 Glahn B, Taylor A, Kurkowski N, Shaffer WA (2009) The role of the SLOSH model in National
848 Weather Service storm surge forecasting. Natl Weather Dig 33(1):3–14.

Gori A, Lin N, Xi D, Emanuel K (2022) Tropical cyclone climatology change greatly exacerbates US extreme rainfall–surge hazard. Nat Clim Change 12(2):171–178. https://doi.org/10.21203/rs.3.rs-805581/v1

Gori A, Lin N, Chavas D, Oppenheimer M, Xian S (2025) Sensitivity of tropical cyclone risk across the US to changes in storm climatology and socioeconomic growth. Environ Res Lett 20(6):064050. https://doi.org/10.1088/1748-9326/add60d

Jelesnianski CP (1992) SLOSH: Sea, lake, and overland surges from hurricanes. Vol. 48. US Department of Commerce, National Oceanic and Atmospheric Administration, National Weather Service. https://vlab.noaa.gov/web/mdl/slosh

Jing R, Heft-Neal S, Chavas DR, Griswold M, Wang Z, Clark-Ginsberg A, Guha-Sapir D, Bendavid E, Wagner Z (2024) Global population profile of tropical cyclone exposure from 2002 to 2019. Nature 626(7999):549–554. https://doi.org/10.1038/s41586-023-06963-z

Jonkman SN, Maaskant B, Boyd E, Levitan ML (2009) Loss of life caused by the flooding of New Orleans after Hurricane Katrina: analysis of the relationship between flood characteristics and mortality. Risk Anal 29(5):676–698. https://doi.org/10.1111/j.1539-6924.2008.01190.0

Helderop E, Grubesic TH (2022) Hurricane storm surge: toward a normalized damage index for coastal regions. Nat Hazards 110(2):1179–1197. https://doi.org/10.1007/s11069-021-04987-0

Henry EH, Burford Reiskind MO, Land AD, Haddad NM (2020) Maintaining historic disturbance regimes increases species' resilience to catastrophic hurricanes. Glob Change Biol 26(2):798–806. https://doi.org/10.1111/gcb.14932

872 Hernández ML, Carreño ML, Castillo L (2018) Methodologies and tools of risk management:
873 Hurricane risk index (HRi). Int J Disaster Risk Reduct 31:926–937.
874 https://doi.org/10.1016/j.ijdrr.2018.08.006
875 Huang H, Fischella MR, Liu Y, Ban Z, Fayne JV, Li D, Cavanaugh KC, Lettenmaier DP (2022)
876 Changes in mechanisms and characteristics of western US floods over the last sixty years.
877 Geophys Res Lett 49(3):e2021GL097022. https://doi.org/10.1029/2021GL097022
878 Huntsman SR (2011) Design and construction of the Lake Borgne surge barrier in response to
879 Hurricane Katrina. In: Coastal engineering practice. ASCE, Reston, pp 117–130.
880 Kaly U, Briguglio L, McLeod H, Schmall S, Pratt C, Pal R (1999) Environmental Vulnerability
881 Index (EVI) to summarise national environmental vulnerability profiles.
882 Kirkland JL, Zick SE (2019) Regional differences in the spatial patterns of North Atlantic
883 tropical cyclone rainbands through landfall. Southeast Geogr 59(3):294–320.
884 https://doi.org/10.1353/sgo.2019.0023
885 Knapp KR, Kruk MC, Levinson DH, Diamond HJ, Neumann CJ (2010) The international best
886 track archive for climate stewardship (IBTrACS) unifying tropical cyclone data. Bull Am
887 Meteorol Soc 91(3):363–376. https://doi.org/10.1175/2009BAMS2755.1
888 Knight DB, Davis RE (2009) Contribution of tropical cyclones to extreme rainfall events in the
889 southeastern United States. J Geophys Res Atmos 114(D23): D23102.
890 https://doi.org/10.1029/2009JD012511
891 Krichene H, Vogt T, Piontek F, Geiger T, Schötz C, Otto C (2023) The social costs of tropical
892 cyclones. Nat Commun 14(1):7294. https://doi.org/10.1038/s41467-023-43114-4

893 Kunkel KE, Easterling DR, Kristovich DA, Gleason B, Stoecker L, Smith R (2010) Recent
894 increases in US heavy precipitation associated with tropical cyclones. Geophys Res Lett
895 37(24):1–4. https://doi.org/10.1029/2010GL045164
896 Lamers A, Sharma M, Berg R, Gálvez JM, Yu Z, Kriat T, Cardos S, Grant D, Moron LA (2023)
897 Forecasting tropical cyclone rainfall and flooding hazards and impacts. Trop Cyclone Res
898 Rev 12(2):100–112. https://doi.org/10.1016/j.tcrr.2023.06.005
899 Liu M, Smith JA (2016) Extreme rainfall from landfalling tropical cyclones in the eastern United
900 States: Hurricane Irene. J Hydrometeorol 17(11):2883–2904.
901 https://doi.org/10.1175/JHM-D-16-0072.1
902 Lumbroso DM, Suckall NR, Nicholls RJ, White KD (2017) Enhancing resilience to coastal
903 flooding from severe storms in the USA: international lessons. Nat Hazards Earth Syst
904 Sci 17(8):1357–1373. https://doi.org/10.5194/nhess-17-1357-2017
905 McDonald JR, Mehta KC, Smith DA, Womble JA (2010) The enhanced Fujita scale:
906 Development and implementation. In: Forensic engineering 2009: Pathology of the built
907 environment, pp 719–728. https://doi.org/10.1061/41082(362)73
908 Manson S, Schroeder J, Van Riper D, Knowles K, Kugler T, Roberts F, Ruggles S (2024)
909 IPUMS National Historical Geographic Information System: Version 19.0.
910 http://doi.org/10.18128/D050.V19.0
911 Marchi L, Borga M, Preciso E, Gaume E (2010) Characterisation of selected extreme flash
912 floods in Europe and implications for flood risk management. J Hydrol 394(1–2):118–
913 133. https://doi.org/10.1016/j.jhydrol.2010.07.017

914 Matyas CJ, Tang J, Comstock IJ, Zick SE (2016) A spatial analysis of Hurricane Katrina's outer
915 rainbands prior to landfall in Louisiana. 2822(375):1–98.
916 https://doi.org/10.13140/RG.2.1.1680.7447
917 Maxwell JT, Bregy JC, Robeson SM, Knapp PA, Soulé PT, Trouet V (2021) Recent increases in
918 tropical cyclone precipitation extremes over the US east coast. Proc Natl Acad Sci USA
919 118(41):e2105636118. https://doi.org/10.1073/pnas.2105636118
920 Mendelsohn R, Zheng L (2020) Coastal resilience against storm surge from tropical cyclones.
921 Atmosphere 11(7):725. https://doi.org/10.3390/atmos11070725
922 Moore TW, Dixon RW (2012) Tropical cyclone-tornado casualties. Nat Hazards 61(2):621–634.
923 https://doi.org/10.1007/s11069-011-0050-z
924 Moore W, Elliott W, Lorde T (2017) Climate change, Atlantic storm activity and the regional
925 socio-economic impacts on the Caribbean. Environ Dev Sustain 19(2):707–726.
926 Morrow BH, Lazo JK, Rhome J, Feyen J (2015) Improving storm surge risk communication:
927 Stakeholder perspectives. Bull Am Meteorol Soc 96(1):35–48.
928 https://doi.org/10.1175/BAMS-D-13-00197.1
929 Mudd L, Rosowsky D, Letchford C, Lombardo F (2017) Joint probabilistic wind–rainfall model
930 for tropical cyclone hazard characterization. J Struct Eng 143(3):04016195.
931 https://doi.org/10.1061/(ASCE)ST.1943-541X.0001685
932 Muller RA, Stone GW (2001) A climatology of tropical storm and hurricane strikes to enhance
933 vulnerability prediction for the southeast US coast. J Coast Res 17(4):949–956
934 Needham HF, Keim BD (2012) A storm surge database for the US Gulf Coast. Int J Climatol
935 32(14):2108–2123. https://doi.org/10.1002/joc.2425

936 Needham HF, Keim BD (2014) Correlating storm surge heights with tropical cyclone winds at
937 and before landfall. Earth Interact 18(7):1–26. https://doi.org/10.1175/2013EI000527.1
938 Nielsen ER, Herman GR, Tournay RC, Peters JM, Schumacher RS (2015) Double impact: When
939 both tornadoes and flash floods threaten the same place at the same time. Weather
940 Forecast 30(6):1673–1693. https://doi.org/10.1175/WAF-D-15-0084.1
941 National Hurricane Center (NHC) (2025) Tropical cyclone reports, Atlantic basin, 2025.
942 https://www.nhc.noaa.gov/data/tcr/index.php?season=2025&basin=atl. Accessed 10 Jan
943 2025
944 NOAA National Centers for Environmental Information (NCEI) (2025) U.S. Billion-Dollar
945 Weather and Climate Disasters. https://www.ncei.noaa.gov/access/billions/
946 National Oceanic and Atmospheric Administration (NOAA) (n.d.) Precipitation data access.
947 NOAA Water. Accessed 19 Jan 2025. https://water.noaa.gov/about/precipitation-data-
948 access
949 National Weather Service (NWS) (n.d.) Hurricane Florence (2018). Weather.gov. Accessed 10
950 Sep 2025. https://www.weather.gov/ilm/hurricaneflorence
951 National Hurricane Center (NHC) (2024) Tropical Cyclone Report: Hurricane Helene
952 (AL092024). Accessed 5 Apr 2025.
953 https://www.nhc.noaa.gov/data/tcr/AL092024_Helene.pdf
954 Paredes M, Schenkel BA, Edwards R, Coniglio M (2021) Tropical cyclone outer size impacts the
955 number and location of tornadoes. Geophys Res Lett 48(24):e2021GL095922.
956 https://doi.org/10.1029/2021GL095922

957 Parks RM, Benavides J, Anderson GB, Nethery RC, Navas-Acien A, Dominici F, Ezzati M,
958 Kioumourtzoglou MA (2022) Association of tropical cyclones with county-level
959 mortality in the US. JAMA 327(10):946–955. https://doi.org/10.1001/jama.2022.1682
960 Paxton CH, Collins JM (2014) Weather, ocean, and social aspects associated with rip current
961 deaths in the United States. J Coast Res 72:50–55. https://doi.org/10.2112/SI72-010.1
962 Peduzzi P (2006) The disaster risk index: overview of a quantitative approach. In: Measuring
963 vulnerability to natural hazards: towards disaster resilient societies, pp 171–181
964 Peduzzi P, Chatenoux B, Dao H, De Bono A, Herold C, Kossin J, Mouton F, Nordbeck O (2012)
965 Global trends in tropical cyclone risk. Nat Clim Change 2(4):289–294.
966 https://doi.org/10.1038/nclimate1410
967 Pilkington SF, Mahmoud HN (2017) Real-time application of the multihazard hurricane impact
968 level model for the Atlantic Basin. Front Built Environ 3:67.
969 https://doi.org/10.3389/fbuil.2017.00067
970 Pyles L (2011) Toward sustainable post-Katrina recovery: Lessons learned from African
971 American neighborhoods. Fam Soc 92(3):344–349. https://doi.org/10.1606/1044-
972 3894.4134
973 Rahmstorf S (2017) Rising hazard of storm-surge flooding. Proc Natl Acad Sci USA
974 114(45):11806–11808. https://doi.org/10.1073/pnas.1715895114
975 Rappaport EN (2000) Loss of life in the United States associated with recent Atlantic tropical
976 cyclones. Bull Am Meteorol Soc 81(9):2065–2074. https://doi.org/10.1175/1520-
977 0477(2000)081

978 Rappaport EN (2014) Fatalities in the United States from Atlantic tropical cyclones: New data
979 and interpretation. Bull Am Meteorol Soc 95(3):341–346.
980 https://doi.org/10.1175/BAMS-D-12-00074.1
981 Rappaport EN, Blanchard BW (2016) Fatalities in the United States indirectly associated with
982 Atlantic tropical cyclones. Bull Am Meteorol Soc 97(7):1139–1148.
983 https://doi.org/10.1175/BAMS-D-15-00042.1
984 Resio DT, Irish JL (2015) Tropical cyclone storm surge risk. Curr Clim Change Rep 1(2):74–84.
985 https://doi.org/10.1007/s40641-015-0011-9
986 Rezapour M, Baldock TE (2014) Classification of hurricane hazards: The importance of rainfall.
987 Weather Forecast 29(6):1319–1331. https://doi.org/10.1175/WAF-D-14-00014.1
988 Rumbach A, Sullivan E, Makarewicz C (2020) Mobile home parks and disasters: Understanding
989 risk to the third housing type in the United States. Nat Hazards Rev 21(2):05020001.
990 https://doi.org/10.1061/(ASCE)NH.1527-6996.0000357
991 Sajjad M, Lin N, Chan JC (2020) Spatial heterogeneities of current and future hurricane flood
992 risk along the US Atlantic and Gulf coasts. Sci Total Environ 713:136704.
993 https://doi.org/10.1016/j.scitotenv.2020.136704
994 Schmidt S, Kemfert C, Höppe P (2010) The impact of socio-economics and climate change on
995 tropical cyclone losses in the USA. Reg Environ Change 10(1):13–26.
996 https://doi.org/10.1007/s10113-008-0082-4
997 Schultz LA, Cecil DJ (2009) Tropical cyclone tornadoes, 1950–2007. Mon Weather Rev
998 137(10):3471–3484. https://doi.org/10.1175/2009MWR2896.1
999 Senkbeil JC, Brommer DM, Comstock IJ (2011) Tropical cyclone hazards in the USA. Geogr
1000 Compass 5(8):544–563. https://doi.org/10.1111/j.1749-8198.2011.00439.x

1001 Shaffer GP, Day JW Jr, Mack S, Kemp GP, van Heerden I, Poirrier MA, Westphal KA,
1002 FitzGerald D, Milanes A, Morris CA, Bea R (2009) The MRGO navigation project: a
1003 massive human-induced environmental, economic, and storm disaster. J Coast Res
1004 10054:206–224. https://doi.org/10.2112/SI54-004.1
1005 Sheng C, Hong HP (2020) On the joint tropical cyclone wind and wave hazard. Struct Saf
1006 84:101917. https://doi.org/10.1016/j.strusafe.2019.101917
1007 Sohn W, Kim JH, Li MH, Brown RD, Jaber FH (2020) How does increasing impervious surfaces
1008 affect urban flooding in response to climate variability? Ecol Indic 118:106774.
1009 https://doi.org/10.1016/j.ecolind.2020.106774
1010 Song JY, Chung ES (2024) Increasing wind threat of Atlantic tropical cyclones based on a
1011 comprehensive risk analysis using Multi-Hazard Hurricane Index and Social
1012 Vulnerability Index. Earth Syst Environ 8(4):951–962. https://doi.org/10.1007/s41748-
1013 024-00471-4
1014 Strader SM, Ashley WS (2018) Finescale assessment of mobile home tornado vulnerability in
1015 the central and southeast United States. Weather Clim Soc 10(4):797–812.
1016 https://doi.org/10.1175/WCAS-D-18-0060.1
1017 Storm Prediction Center (2025) Tropical Cyclone Tornadoes. National Oceanic and Atmospheric
1018 Administration, Norman, OK. https://www.spc.noaa.gov/exper/tctor/
1019 Summers JK, Lamper A, McMillion C, Harwell LC (2022) Observed changes in the frequency,
1020 intensity, and spatial patterns of nine natural hazards in the United States from 2000 to
1021 2019. Sustainability 14(7):4158. https://doi.org/10.3390/su14074158
1022 Swain ED, Bellino JC (2022) Insight into Hurricane Maria peak daily streamflows from the
1023 development and application of the Precipitation-Runoff Modeling System (PRMS):

1024 including Río Grande de Arecibo, Puerto Rico, 1981–2017. Hydrology 9(11):205.
1025 https://doi.org/10.3390/hydrology9110205
1026 Tan C, Fang W (2018) Mapping the wind hazard of global tropical cyclones with parametric
1027 wind field models by considering the effects of local factors. Int J Disaster Risk Sci
1028 9(1):86–99. https://doi.org/10.1007/s13753-018-0161-1
1029 Tennille SA, Ellis KN (2017) Spatial and temporal trends in the location of the lifetime
1030 maximum intensity of tropical cyclones. Atmosphere 8(10):198.
1031 https://doi.org/10.3390/atmos8100198
1032 Thywissen K (2006) Core terminology of disaster reduction: A comparative glossary. In:
1033 Measuring vulnerability to natural hazards: Towards disaster resilient societies, pp 448–
1034 496
1035 Tonn G, Czajkowski J (2022) US tropical cyclone flood risk: Storm surge versus freshwater.
1036 Risk Anal 42(12):2748–2764. https://doi.org/10.1111/risa.13890
1037 Touma D, Stevenson S, Camargo SJ, Horton DE, Diffenbaugh NS (2019) Variations in the
1038 intensity and spatial extent of tropical cyclone precipitation. Geophys Res Lett
1039 46(23):13992–14002. https://doi.org/10.25349/D9F30M
1040 Towey KL, Booth JF, Enriquez AR, Wahl T (2022) Tropical cyclone storm surge probabilities
1041 for the east coast of the United States: a cyclone-based perspective. Nat Hazards Earth
1042 Syst Sci 22(4):1287–1300. https://doi.org/10.5194/nhess-2021-251
1043 Trepanier JC, Yuan J, Jagger TH (2017) The combined risk of extreme tropical cyclone winds
1044 and storm surges along the US Gulf of Mexico Coast. J Geophys Res Atmos
1045 122(6):3299–3316. https://doi.org/10.1002/2016JD026180

United Nations Office for Disaster Risk Reduction (UNDRR) (2017) The Sendai Framework Terminology on Disaster Risk Reduction. "Exposure". https://www.undrr.org/terminology/exposure

United Nations Office for Disaster Risk Reduction (UNDRR) (2017) The Sendai Framework Terminology on Disaster Risk Reduction. "Vulnerability". https://www.undrr.org/terminology/vulnerability

United Nations Office for Disaster Risk Reduction (UNDRR) (2017) The Sendai Framework Terminology on Disaster Risk Reduction. "Resilience". https://www.undrr.org/terminology/resilience

United Nations Office for Disaster Risk Reduction (UNDRR) (2017) The Sendai Framework Terminology on Disaster Risk Reduction. "Disaster risk". Accessed 30 August 2025. https://www.undrr.org/terminology/disaster-risk

Van Oldenborgh GJ, Van Der Wiel K, Sebastian A, Singh R, Arrighi J, Otto F, Haustein K, Li S, Vecchi G, Cullen H (2017) Attribution of extreme rainfall from Hurricane Harvey, August 2017. Environ Res Lett 12(12):124009. https://doi.org/10.1088/1748-9326/aa9ef2

Varlas G, Papadopoulos A, Katsafados P (2019) An analysis of the synoptic and dynamical characteristics of hurricane Sandy (2012). Meteorol Atmos Phys 131(3):443–453. https://doi.org/10.1007/s00703-017-0577-y

Villarini G, Goska R, Smith JA, Vecchi GA (2014) North Atlantic tropical cyclones and US flooding. Bull Am Meteorol Soc 95(9):1381–1388. https://doi.org/10.1175/BAMS-D-13-00060.1

1067 Wilson KM, Baldwin JW, Young RM (2022) Estimating tropical cyclone vulnerability: A review
1068 of different open-source approaches. In: Hurricane Risk in a Changing Climate, 2:255–
1069 281. https://doi.org/10.1007/978-3-031-08568-0_11
1070 Xi D, Lin N (2022) Investigating the physical drivers for the increasing tropical cyclone rainfall
1071 hazard in the United States. Geophys Res Lett 49(15):e2022GL099196.
1072 https://doi.org/10.1029/2022GL099196
1073 Xiao YF, Duan ZD, Xiao YQ, Ou JP, Chang L, Li QS (2011) Typhoon wind hazard analysis for
1074 southeast China coastal regions. Struct Saf 33(4–5):286–295.
1075 https://doi.org/10.1016/j.strusafe.2011.04.003
1076 Young R, Hsiang S (2024) Mortality caused by tropical cyclones in the United States. Nature
1077 635(8037):121–128. https://doi.org/10.1038/s41586-024-07945-5
1078 Zachry BC, Booth WJ, Rhome JR, Sharon TM (2015) A national view of storm surge risk and
1079 inundation. Weather Clim Soc 7(2):109–117. https://doi.org/10.1175/WCAS-D-14-
1080 00049.1